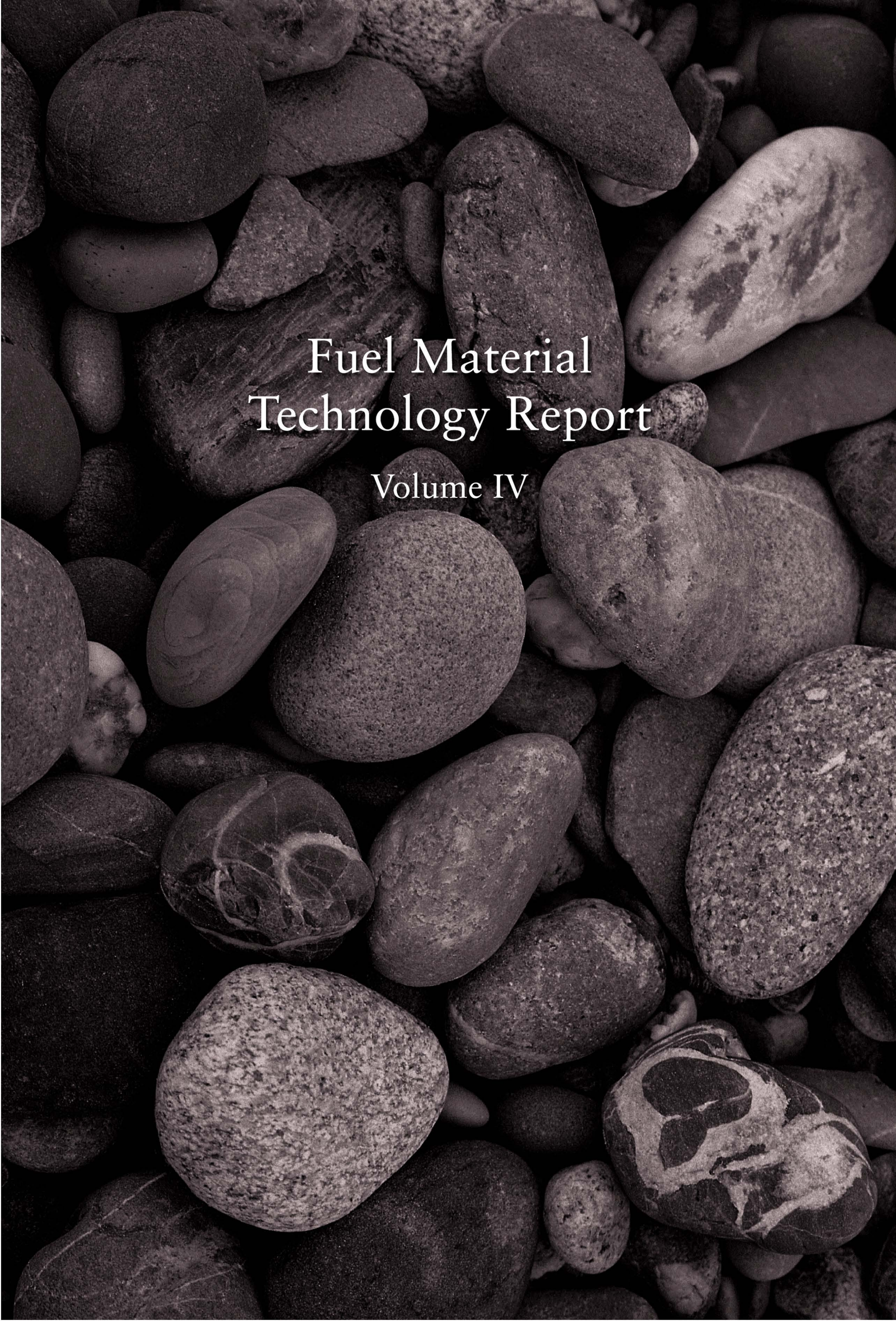

Fuel Material Technology Report

Volume IV

FUEL MATERIAL TECHNOLOGY REPORT

Volume IV

Authors

Peter Rudling
ANT International, Skultuna, Sweden

Charles Patterson
Clovis, CA, USA

A.N.T. INTERNATIONAL®

Advanced Nuclear Technology International
Krongjutarvägen 2C, SE-730 50 Skultuna
Sweden

info@antinternational.com
www.antinternational.com

Disclaimer

The information presented in this report has been compiled and analysed by Advanced Nuclear Technology International Europe AB (ANT International®) and its subcontractors. *ANT* International has exercised due diligence in this work, but does not warrant the accuracy or completeness of the information. *ANT* International does not assume any responsibility for any consequences as a result of the use of the information for any party, except a warranty for reasonable technical skill, which is limited to the amount paid for this assignment by each Project programme member.

Acknowledgements

The authors would like to thank both Ringhals and OKG-E.ON for their willingness to provide photos of Fuel Assembly (*FA*) components.

Acronyms and expressions

ANT	Advanced Nuclear Technology
AOA	Axial Offset Anomaly
AOO	Anticipated Operational Occurrence
APSR	Axial Power Shaping Rods
AR	Annual Report
ASTM	American Society for Testing and Materials
B&W	Babcock & Willcox
BEI	Backscattered Electron Imaging
BOC	Beginning of Cycle
BWR	Boiling Water Reactor
CANDU	Canadian Deuterium Uranium
CHF	Critical Heat Flux
CILC	*CRUD* Induced Localised Corrosion
CRUD	Chalk River Unidentified Deposits
CW	Cold Worked
DCP	Distinctive *CRUD* Pattern
DNB	Departure from Nucleate Boiling
DZO	Depleted Zinc Oxide
EC	Eddy Current
ECR	Equivalent Cladding Reacted
ECT	Eddy Current Testing
EDS	Energy Dispersive Spectroscopy
EDXS	Energy Dispersive X-ray Spectroscopy
ELS	Extra-Low Sn
EOC	End Of Cycle
EPMA	Electron Probe Micro Analysis
ESSC	Enhanced Spacer Shadow Corrosion
FA	Fuel Assembly
FGR	Fission Gas Release
FM	Fissionable Materials
FMTR	Fuel Material Technology Report
GE	General Electric
GETR	General Electric Test Reactor
GNF	Global Nuclear Fuel
HBS	High Burnup Structure
HFE	Healthy Fuel Examinations
HPA	High Performance Alloy
HPUF	Hydrogen PickUp Fraction
HWC	Hydrogen Water Chemistry
IAEA	International Atomic Energy Agency
ICPMS	Inductively Coupled Plasma Mass Spectrometry
ID	Inner Diameter
IFM	Intermediate Flow Mixers
INPO	Institute of Nuclear Power Operations
IZNA	International Atomic Energy Agency
KKL	KernKraftwerk Leibstadt
KWO	KernKraftwerk Obrigheim
KWU	KraftWerkUnion
LAF	Laser-Flash

LCC	*LWR* Coolant Chemistry
LECO	Corporation provides instrumentation for elemental determination in organic and inorganic materials
LHGR	Linear Heat Generation Rate
LK	Låg corrosion (Low Corrosion in Swedish)
LME	Liquide Metal Embrittlement
LOCA	Loss of Coolant Accident
LVDT	Linear Variable Differential Transducer
LWR	Light Water Reactor
MDA	Mitsubishi Developed Alloy
MHI	Mitsubishi Heavy Industries
MOX	Mixed OXide
NDA	New Developed Alloy
NEA	Nuclear Energy Agency
NFI	Nuclear Fuel Industries
NMCA	Noble Metal Chemical Addition
NPP	Nuclear Power Plant
NWC	Normal Water Chemistry
OD	Outer Diameter
PCI	Pellet Cladding Interaction
PCIOMR	Preconditioning Interim Operating Management Recommendations
PCMI	Pellet Cladding Mechanical Interaction
PCT	Peak Cladding Temperature
PGS	Pickering Generation Station
PIE	Post-Irradiation Examinations
PWR	Pressurised Water Reactor
QA	Quality Assurance
QC	Quality Control
RBMK	Reaktor Bolshoi Mozhnosti Kanalov (in English Large Boiling Water Channel type reactor)
RCCA	Rod Cluster Control Assembly
RFA	Robust Fuel Assembly
RIA	Reactivity Initiated Accident
RPV	Reactor Pressure Vessel
RXA	Recrystallised Annealed
SCC	Stress Corrosion Cracking
SEM	Scanning Electron Microscopy: generally operated at accelerating voltages < 40 kV, it relies on scanning a small electron probe on the sample surface to produce the signal (image) with a resolution of ~1 nm in a field emission SEM; the same probe can be used to excite X-rays for Energy Dispersive X-ray Spectroscopy (*EDXS*) analysis of the same regions with ~1 mm spatial resolution.
SIMFEX	SIMulated Fuel EXpansion
SIMS	Secondary Ion Mass Spectroscopy
SPP	Second Phase Particle
SRA	Stress Relieved Annealed
SS	Stainless Steel
STP	Standard Temperature and Pressure
STR	Special Topic Report
TE	Total Elongation
TEM	Transmission Electron Microscopy: generally operated at accelerating voltages >100 kV, it has the ability to illuminate a wide area of the sample to form an image with resolutions approaching 0.1 nm, or focus the probe to obtain *EDXS* spectra from small areas; it also has the ability to provide electron diffraction data from the same areas.
TFGR	Transient Fission Gas Release
TIG	Tungsten Inert Gas
TMI	Three Mile Island

UE	Uniform Elongation
UT	Ultrasonic Testing
UTS	Ultimate Tensile Strength
VVER	Voda Voda Energo Reactor (Russian type *PWR*)
XPS	X-ray Photoelectron Spectroscopic
YS	Yield Strength
ZIRAT	ZIRconium Alloy Technology
ZIRLO	ZIRconium Low Oxidation

Unit conversion

TEMPERATURE		
°C + 273.15 = K		°C*1.8 +32 = °F
T(K)	T(°C)	T(°F)
273	**0**	32
289	16	61
298	25	77
373	**100**	212
473	**200**	392
573	**300**	572
633	360	680
673	**400**	752
773	**500**	932
783	510	950
793	520	968
823	550	1022
833	560	1040
873	**600**	1112
878	605	1121
893	620	1148
923	650	1202
973	**700**	1292
1023	750	1382
1053	780	1436
1073	**800**	1472
1136	863	1585
1143	870	1598
1173	**900**	1652
1273	**1000**	1832
1343	1070	1958
1478	1204	**2200**

Radioactivity	
1 Sv	= 100 Rem
1 Ci	= 3.7 x 10^{10} Bq = 37 GBq
1 Bq	= 1 s^{-1}

MASS	
kg	lbs
0.454	**1**
1	2.20

DISTANCE	
x (µm)	x (mils)
0.6	0.02
1	0.04
5	0.20
10	0.39
20	0.79
25	0.98
25.4	**1.00**
100	3.94

PRESSURE		
bar	MPa	psi
1	0.1	14
10	**1**	142
70	7	995
70.4	7.04	**1000**
100	10	1421
130	13	1847
155	15.5	2203
704	70.4	**10000**
1000	100	14211

STRESS INTENSITY FACTOR	
MPa√m	ksi√inch
0.91	**1**
1	1.10

Contents

Acknowledgements		**II**
Acronyms and expressions		**III**
Unit conversion		**VI**
1	**Introduction**	**1-1**
2	**Structure and components of the *BWR* and *PWR FA***	**2-1**
3	**Impact of irradiation on fuel performance**	**3-1**
3.1	Introduction	3-1
3.2	Fuel pellet	3-3
3.3	Zr alloy materials	3-8
3.3.1	Irradiation damage	3-8
3.3.2	Corrosion	3-10
3.3.2.1	Temperature and temperature history impact	3-14
3.3.2.2	Materials (zirconium alloys) impact	3-17
3.3.2.3	Hydrogen impact	3-17
3.3.2.4	Water chemistry and boiling duty impact	3-19
3.3.3	Ductility	3-21
3.3.4	*PCI/PCMI*	3-22
3.3.5	Dimensional changes	3-24
3.3.5.1	Introduction	3-24
4	**Fuel vendor licensing data**	**4-1**
5	**Root cause examinations of failed and degraded fuel**	**5-1**
5.1	Introduction	5-1
5.2	Detection and assessment of defected fuel during operation	5-4
5.2.1	Sipping	5-11
5.2.2	*UT*	5-16
5.3	Classification of primary failure causes	5-18
5.3.1	Duty related failures – *PCI/PCMI*	5-18
5.3.1.1	Introduction	5-18
5.3.1.2	Information collected before outage	5-24
5.3.1.3	Information collected during poolside fuel examinations	5-25
5.3.1.4	Information during hotcell fuel examinations	5-28
5.3.2	Non-duty related failures	5-31
5.3.2.1	Debris fretting	5-31
5.3.2.2	Information collected before outage	5-32
5.3.2.3	Information collected during poolside fuel examinations	5-33
5.3.2.3.1	Information during hotcell fuel examinations	5-34
5.3.2.4	Manufacturing defects (welding defects, end plug piping and primary hydriding)	5-34
5.3.2.4.1	Information collected before outage	5-35
5.3.2.4.2	Information collected during poolside fuel examinations	5-36
5.3.2.4.3	Information during hotcell fuel examinations	5-36
5.3.2.5	Grid-to-rod fretting	5-36
5.3.2.6	Information collected before outage	5-38
5.3.2.6.1	Information collected during poolside fuel examinations	5-38
5.3.2.6.2	Information during hotcell fuel examinations	5-38
5.3.2.7	Corrosion	5-39
5.3.2.7.1	Information collected before outage	5-42
5.3.2.7.1.1	Information collected during poolside fuel examinations	5-43
5.3.2.7.2	Information during hotcell fuel examinations	5-44
5.4	Degradation of failed fuel	5-46

5.4.1	Introduction	5-46
5.4.2	*BWR* secondary degradation	5-48
5.4.3	*PWR* secondary degradation	5-52
5.4.4	Inspection of failed and degraded fuel	5-53
6	**Maintaining good fuel reliability, *HFE***	**6-1**
7	***FA* characterisation techniques**	**7-1**
7.1	*FA* outer flow channel (*BWR*)	7-2
7.2	*FA*	7-6
7.3	Fuel rod	7-10
7.3.1	Poolside examination	7-10
7.3.2	Hot cell examination	7-18
7.4	Grid/spacer and guide tube	7-33
7.4.1	Poolside examination	7-33
7.4.2	Hot cell examination	7-35
8	**References**	**8-1**

1 Introduction

The primary objective of this volume of the Fuel Material Technology Report (*FMTR*) Vol. 4 is to provide guidance in improving fuel reliability. To reach this objective various Poolside and Hot Cell Examinations techniques may be used. A good knowledge of the pros- and cons- with the different techniques can guide the utility/fuel vendor to select the most cost efficient techniques for this specific objective. A second objective of this Report is to document this knowledge in a form, which can be updated as new information, and methods become available.

There are several reasons why poolside and/or hot cell examinations are done on *FA* components. The reasons are:

1) Root cause investigations of failed *FA* components, which has degraded, or not.
   a) A "failed" *FA* component has a wider meaning in this respect. It does not only mean that the component has physically failed but it could also mean that the component does not behave satisfactory, e.g. *FA* bowing that is so large that control rods cannot be inserted.
2) Maintaining good fuel reliability by:
   a) Providing base line data before a change in operational environment of the fuel.
   b) Get early warnings of potential issues.
3) Fuel vendor design and licensing data such as:
   a) Providing data to material models and fuel performance codes.
   b) Verification of the good performance of a new fuel design.
   c) Assessment of the effects of changes in the operating environment; e.g., water chemistry improvements or higher exposures.

The reasons for the examinations, the techniques used and the interpretation of the results are discussed in the following section.

The Report structure is as follows:

- Section 2 provides an introduction to the Pressurised Water Reactor (*PWR*) and Boiling Water Reactor (*BWR*) *FA* structures and structural materials being used
- Section 3 gives an overview of how the neutron irradiation in the core impacts the properties of fuel and zirconium-based alloy materials and affects the performance of *FA* components. The interested reader of this topic is referred to *FMTR* Vol. 1, Cox et al., 2006, and *FMTR Vol.* 2, Rudling et al., 2007, as well as the following ZIRconium Alloy Technology (*ZIRAT*)/International Atomic Energy Agency (*IZNA*) Special Topic Reports (*STR*):
  - **Corrosion & Hydriding Topics**
    - Corrosion of Zirconium Alloys, *ZIRAT7*/*IZNA2*, Adamson et al., 2002/2003.
    - Corrosion of Zr-Nb Alloys in *PWR*s, *ZIRAT9*/*IZNA4*, Cox et al., 2004/2005.
    - Corrosion mechanisms, *ZIRAT12*/*IZNA7*, Adamson et al., 2007/2008.
    - Impact of Water Chemistry and Chalk River Unidentified Deposits (*CRUD*) on Fuel Performance, *ZIRAT6*/*IZNA1*, Wikmark & Cox, 2001/2002.
    - The Effects of Zn Injection (*PWR*s and *BWR*s) and Noble Metal Chemistry (*BWR*s) on Fuel Performance, *ZIRAT8*/*IZNA3*, Cox et al., 2003/2004.
  - **Mechanical Property Topics**
    - Mechanical Properties of Zirconium Alloys, *ZIRAT6*/*IZNA1*, Adamson & Rudling, 2001/2002.
    - Hydriding Mechanisms and Impact on Fuel Performance, *ZIRAT5*/*IZNA1*, Cox & Rudling, 2000.
    - Pellet Cladding Interaction and Pellet Cladding Mechanical Interaction, *ZIRAT11*/*IZNA6*, Adamson et al., 2006/2007.
  - **Manufacturing Topics**
    - Manufacturing of Zirconium Alloy Materials, *ZIRAT5*/*IZNA1*, Rudling & Adamson, 2000.
    - Manufacturing of Zr-Nb alloys, *ZIRAT11*/*IZNA6*, Nikulina et al., 2006/2007.
    - Welding of Zirconium Alloys, *ZIRAT12*/*IZNA7*, Rudling et al., 2007/2008.

  - **Dimensional Changes Topics**
    - Dimensional Instability, *ZIRAT7/IZNA2*, Adamson & Rudling, 2002/2003.
    - Structural Behaviour of Fuel Components, *ZIRAT10/IZNA5*, Cox et al., 2005/2006.
  - **Other Topics**
    - High Burnup Fuel Issues – Their Most Recent Status, *ZIRAT8/IZNA3*, Adamson et al., 2003/2004.
    - Impact of Irradiation on Material Performance, *ZIRAT10/IZNA5*, Adamson & Cox, 2005/2006.
- Section 4 provides information about the type of data fuel vendors need for their fuel performance codes.
- Section 5 discusses the failure characteristics and which type of examination techniques and supporting data are needed to assess the primary failure cause. This section also describes the mechanisms behind degradation of failed fuel and what type of data are needed to obtain a better understanding of why certain rods degrade while other do not.
- Section 6 provides guidelines on how to carry out Healthy Fuel Examinations (*HFE*) in an optimised way.
- Section 7 gives examples of various Poolside and Hot Cell Examination techniques of *FA* components that are currently available.

2 Structure and components of the *BWR* and *PWR FA*

There is a wide variety of different types of fuel assemblies for Light Water Reactors, (*LWRs*), Table 2-1.

Table 2-1: Design parameters in water cooled reactors.

Parameter		Western type *PWR*	*VVER*[1] (440/1000) MW	*BWR*
1.	Coolant	Pressurised H_2O	Pressurised H_2O	Boiling H_2O
2.	*FA* materials (pressure tube materials)	Zr-4, *ZIRLO*[2], DUPLEX, M5, *MDA*[3], *NDA*[4], Inconel, *SS*[5]	E110, E635	Zry-2, Zry-4, Inconel, *SS*
3.	Average power rating, (kW/l)	80-125	83/108	40-57
4.	Fast neutron flux, average, n/cm^2.s	6-9E13	5E13/7E13	4-7E13
5.	Temperature, °C			
	Average coolant inlet	279-294	267/290	272-278
	Average coolant outlet	313-329	298/320	280-300
	Max cladding Outer Diameter (*OD*)	320-350	335/352	285-305
	Steam mass content, %			7-14
6.	System pressure, bar	155-158	125/165	70
7.	Coolant flow, m/s	3-6[6]	3.5/6	2-5[6]
8.	Coolant chemistry			
	Oxygen, ppb	<0.05	<0.1	200-400
	Hydrogen (D_2),			
	ppm	2-4		<1.8[7]
	cc/kg	25-50	30-60	
	Boron (as boric acid), ppm	0-2200	0-1400	-
	Li (as LiOH), ppm	0.5-3.5	0.05-0.6	-
	K (as KOH), ppm	-	5-20	-
	NH_3, ppm		6-30	
	NaOH, ppm		0.03-0.35	

[1] Voda Voda Energo Reactor (Russian type PWR)
[2] ZIRconium Low Oxidation
[3] Mitsubishi Developed Alloy
[4] New Developed Alloy
[5] Stainless Steel
[6] Variation from lower to upper part of the core and from plant to plant
[7] Dependant on whether hydrogen is being added to the feedwater or not.

The fuel rod array for *BWR*s was initially 7x7 but there has been a trend over the years to increase the number of Fuel Assembly (*FA*), rods and today most *FA* designs are either of 9x9 or 10x10 square configuration design. The driving force for this trend was to reduce the Linear Heat Generation Rate (*LHGR*), which resulted in a number of fuel performance benefits such as lower Fission Gas Release (*FGR*), and increased Pellet Cladding Interaction (*PCI*) margins. However, to increase utility competitiveness, the *LHGR*s of 9x9 and 10x10 *FA* has successively been increased, and peak *LHGR*s are today almost comparable to that of the 7x7 and 8x8 older designs.

Also for *PWR*s there has been a trend to greater subdivision of fuel rods, e.g. from Westinghouse 15x15 to 17x17 design, however to accomplish this one had to go to a new reactor design. This since the *PWR*s do not have the same flexibility with core internals and control rods as is the case for *BWR*s. Figure 2-1 shows the current *PWR* fuel rod array designs.

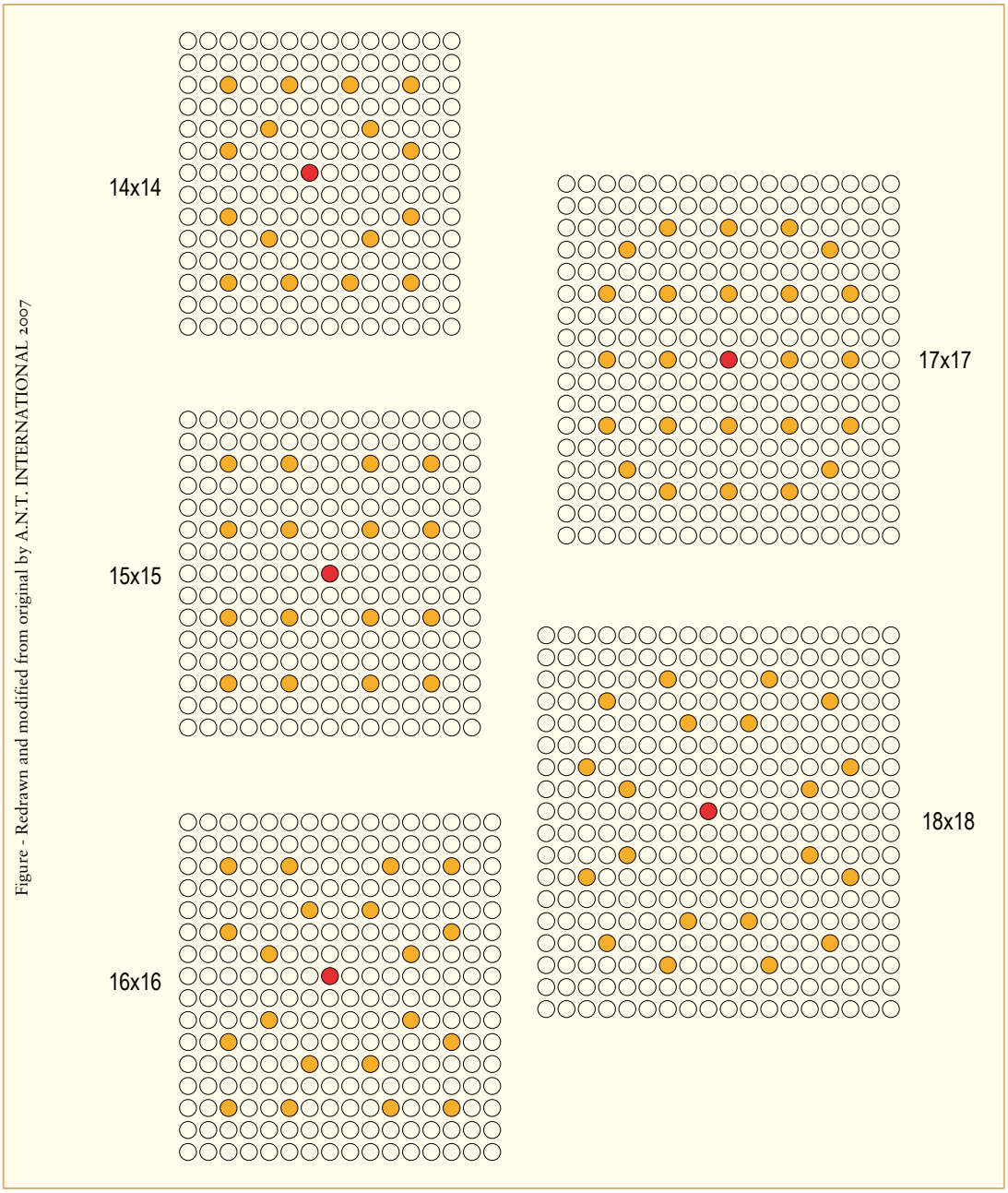

Figure 2-1: Layouts of different *PWR FA* design, rods marked with yellow colour are guide tubes into which the control rod cluster is inserted. The position marked by a red filled circle is the instrument tube position.

In most *PWR*s, the assemblies are positioned in the core by bottom and top fittings, and the lateral clearances are restricted by the assembly-to-assembly contacts at the spacer-grid levels. Furthermore, the control rods consist of Rod Cluster Control Assemblies (*RCCA*s) the poison part of which moves into guide thimbles (or guide tubes). These guide thimbles are an integral part of the assembly structure.

In all *BWR*s, the assemblies are enclosed in "fuel channels" surrounding the assemblies and between which the blades of the control rods moves.

Irrespective of the many possible different shapes, sizes and configurations, the common *FA* design requirements are:

- Maintain proper positioning of the fuel rods under normal operating conditions and in design basis accidents (e.g. seismic effects, Loss of Coolant Accident (*LOCA*), Reactivity Initiated Accident (*RIA*)).
- Permit handling capability before and after irradiation.

Figure 2-2 and Figure 2-3 show a typical *BWR* and *PWR FA*, respectively. Also, the different *FA* components are shown and the material selections for these components are provided. The reason for the difference in structural material selection is that in general the most inexpensive material is chosen for a specific component that yields the lowest cost to produce the component while ensuring adequate performance during normal operation and accidents. More information about fuel designs, functions of the different fuel design components and material being used are provided in *FMTR* Vol. 1, Cox et al., 2006.

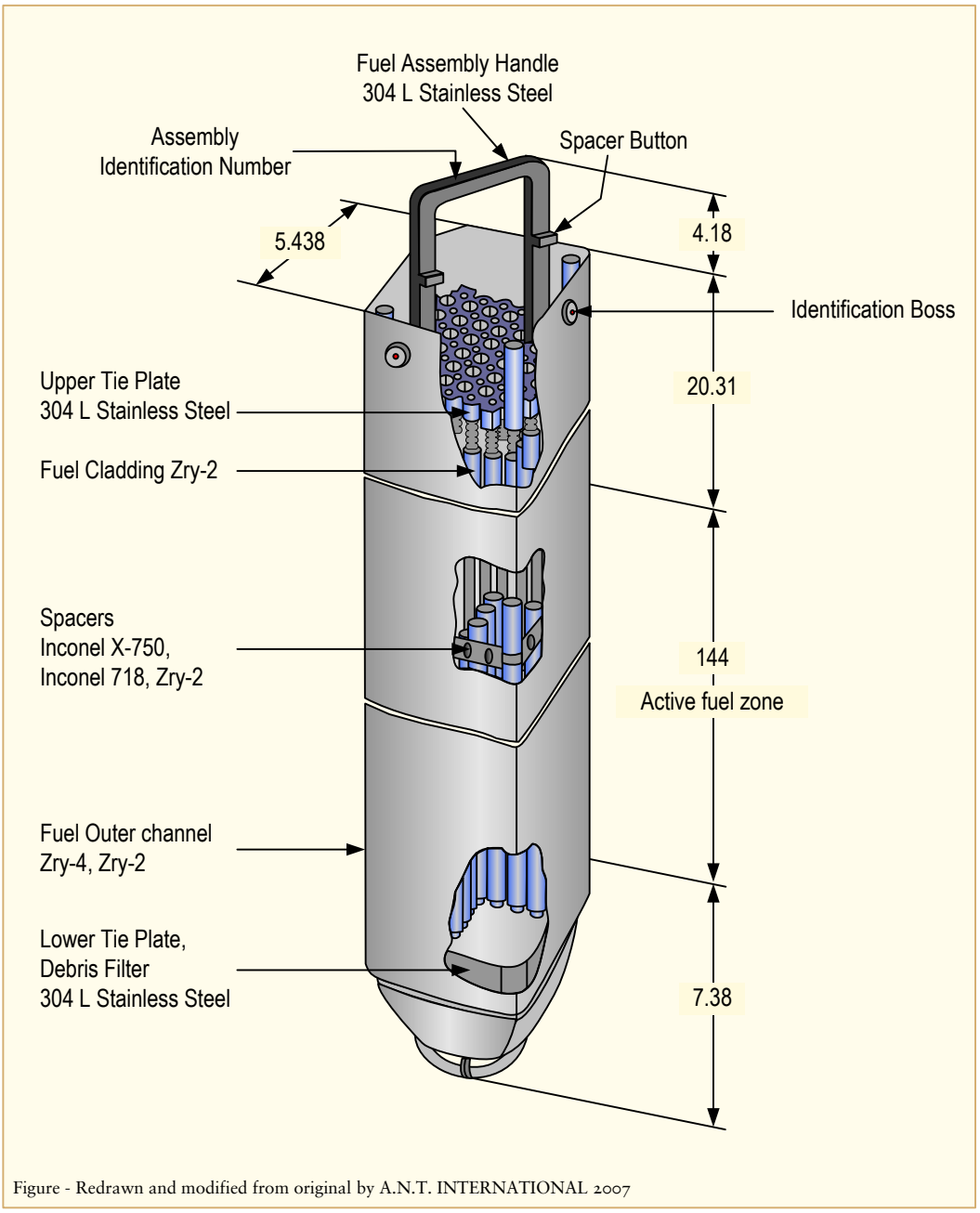

Figure 2-2: Typical *BWR FA* in inches.

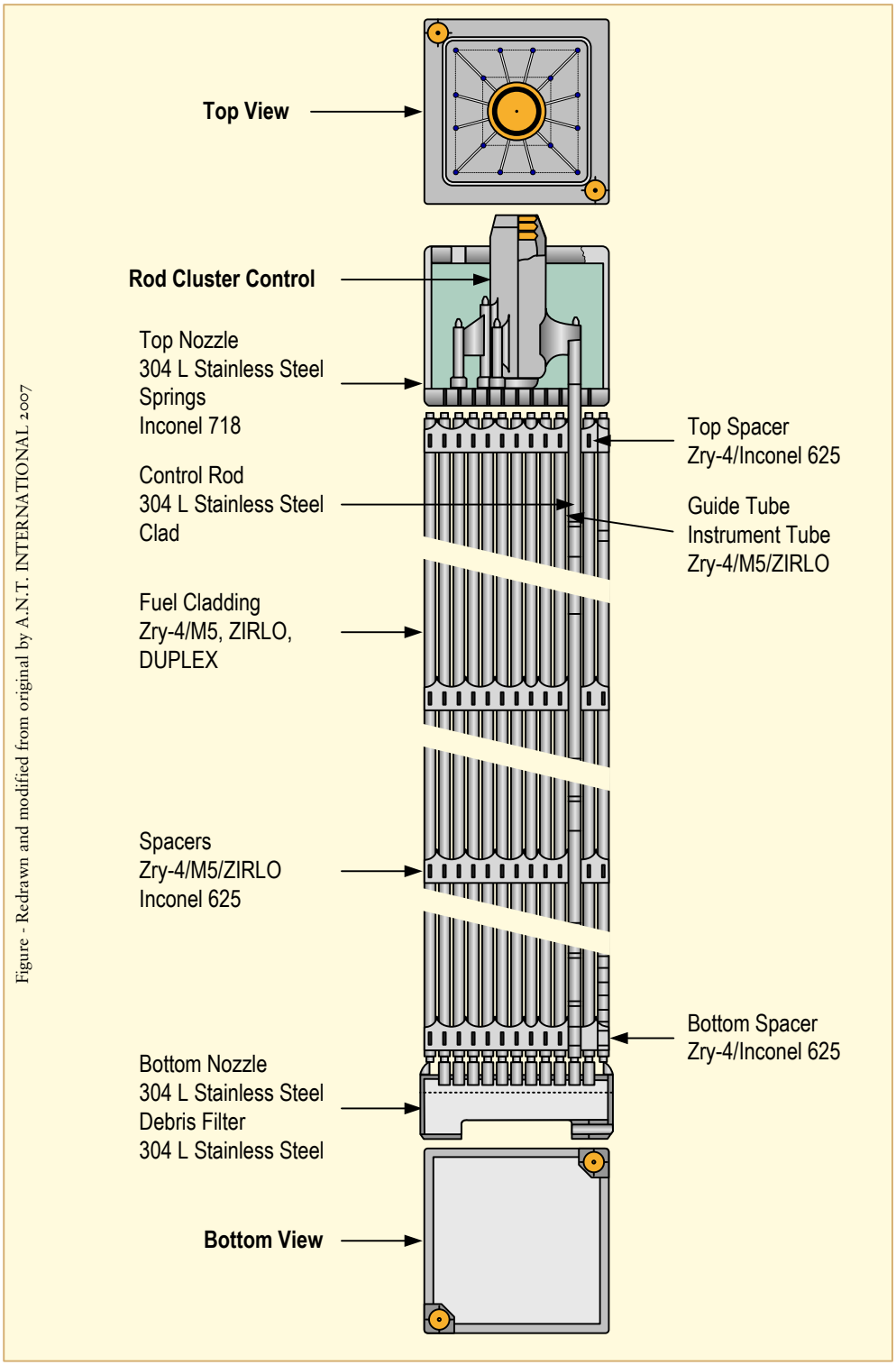

Figure 2-3: Typical *PWR FA*.

The materials used for the *FA* components are Zr alloys, Inconel[1] (precipitation hardened Inconel X-750, Inconel 718 and solution treated Inconel 625) and stainless steel (*SS* 304L or similar austenitic stainless steels). A low cobalt content is desired to keep the radiological exposure of workers (man-rem) low in the stainless steel and nickel-base alloys. However, only Zr alloys have low thermal neutron cross section. Thus, for components in the core mostly Zr alloys are used since the high thermal neutron flux would otherwise result in large loss in reactivity if other materials such as stainless steels and/or nickel-base alloys were used. Spring materials need to be made of materials with low stress relaxation rates, such as e.g. Inconel X-750 or Inconel 718. These Ni base alloys are generally heat treated to reach an optimum precipitation hardening. To lower the parasitic neutron absorption for grids/spacers, the strips are made of Zry-2 and –4, while the spring itself is made of either Inconel X-750 or Inconel 718 to ensure adequate fuel rod support during its entire irradiation. In some fuel designs also the top and bottom *PWR* grid is entirely made of Inconel X-750 or Inconel 718. This is possible since the neutron flux is much lower at the top and bottom part of the core resulting in a very small loss of thermal neutrons due to parasitic material absorption. The low neutron flux at the top and bottom part of the core is also the reason why the much cheaper material *SS* 304 L can be used instead of e.g. Zr alloys for components at these elevations. In newer *BWR* designs the spacers are made entirely of Inconel X-750 or 718, using the minimum thicknesses and minimum planar cross-section possible. Table 2-2 and presents an overview of alloys used in *LWR* and their typical compositions.

Table 2-3 provides data for different Zr alloys used by different fuel vendors. It is noteworthy that there are so many different Zr-alloys for *PWR* applications. Originally Zry-4 was used in *PWR*s but severe corrosion duty resulted in a need to develop more corrosion resistant alloys either as monotubes or as DUPLEX tubes. However, for *BWR*s, the originally selected material, Zry-2, appears to have adequate corrosion performance even today and recent in-pile tests of other Zr alloys have shown that it is difficult to find a material with better corrosion resistance than that of Zry-2. The shift to higher burnup, longer residence fuel designs has, however, led to the development of a number of Zry-2 variants that have been optimized to reduce the pickup of hydrogen in a *BWR* environment; e.g., iron concentrations greater than the normal specification range. Initially Zr-sponge liner was used as a *PCI* remedy for *BWR* applications. It was later found that the Zr sponge material results in a large tendency for secondary degradation of failed fuel and therefore all fuel vendors added some alloying elements to increase the resistance towards secondary degradation of failed rods. The most potent alloying element to obtain this increased resistance is Fe by improving corrosion resistance of the liner material. However, Fe also has a tendency to decrease *PCI* performance.

Table 2-2: Chemical compositions of various stainless steels and Ni base alloys.

Material	Fe (wt%)	Ni (wt%)	Cr (wt%)	Mn (wt%)	Si (wt%)	Mo (wt%)	Ti (wt%)	Nb (wt%)	Al (wt%)
AISI 304	Bal.	10	19	≤2	≤0.75				
DIN 1.4541	Bal.	11	18	≤2	≤0.75		0.4		
Inconel X-750	7	Bal.	15	≤1	≤1		2.6	1	0.7
Inconel 718	17	Bal.	19	0.5	0.75	3	0.7	5	0.6
Inconel 625	2.5	Bal.	22	0.3	0.1	8.8	0.3	3.9[2]	0.2

[1] The name "Inconel" is a registered trademark of the International Nickel Company, which is now the Special Metals Corporation, and refers to their material. Although nickel-based alloys are now produced by a number of suppliers, the name "Inconel" is used instead of a more general designation, such as "alloy X750", for consistency with historic industry practices.
[2] (Nb+Ta) = 3.9 wt%

Table 2-3: Chemical composition of Zr alloys used in *LWR*s.

Alloy	Sn %	Nb %	Fe %	Cr %	Ni %	O %	Fuel Vendor
*BWR*s							
Zircaloy-2	1.2-1.7	-	0.07-0.2	0.05-0.15	0.03-0.08	0.1-0.14	All fuel vendors
Zr-Liner[3]							
Sponge	-	-	0.015-0.06	-	-	0.05-0.1	Only used in Japan and Russia
ZrSn	0.25	-	0.03-0.06	-	-	0.05-0.1	Westinghouse
ZrFe	-	-	0.4	-	-	0.05-0.1	AREVA
ZrFe	-	-	0.10	-	-	0.05-0.1	Global Nuclear Fuel (*GNF*) P7[4]
*PWR*s							
Zircaloy-4	1.2-1.7	-	0.18-0.24	0.07-0.13	-	0.1-0.14	Only used in Japan and France
ZIRLO	1	1	0.1	-	-	0.12	Westinghouse
Optimized *ZIRLO*	0.7	1	0.1	-	-	0.12	Westinghouse
M5	-	0.8-1.2	0.015-0.06	-	-	0.09-0.12	AREVA
High Performance Alloy (*HPA*-4)	0.6	-	Fe+V	-	-	0.12	AREVA
NDA	1	0.1	0.3	0.2		0.12	Nuclear Fuel Industries (*NFI*)
MDA	0.8	0.5	0.2	0.1		0.12	Mitsubishi Heavy Industries (*MHI*)
Duplex[5]							
Extra-Low Sn (*ELS*)[6]	0.5/0.8	-	0.3/0.5	0.2	-	0.12	AREVA
D4	0.5	-	0.7	-	0.12		AREVA
3b[7]	<0.8	-		<0.6			Westinghouse
3b+[8]	<1.0	-		<0.6			Westinghouse
D4[9]	<0.8	-		<0.6			Westinghouse
VVER, Reaktor Bolshoi Mozhnosti Kanalov(*RBMK*)							
E-110	-	0.9-1.1	0.014	<0.003	0.0035	0.05-0.07	Fuel Cladding
Alloy E125	-	2.5	-	-	-	0.06	Pressure tube in *RBMK*
Canadian Deuterium Uranium (*CANDU*)							
Zircaloy-4	1.2-1.7	-	0.18-0.24	0.07-0.13	-	0.1-0.14	Fuel Cladding
Zr2.5Nb	-	2.4-2.8	<0.15	-	-	0.09-0.13	Pressure tube

[3] In all BWR liner cladding tubes about 90 % of the thickness-the outer part of the cladding tube consists of Zry-2.
[4] *GNF* have developed P8 liner that contains somewhat higher Fe content than that of P7 liner
[5] All DUPLEX claddings consist of an outer corrosion resistant layer with a thickness < 100 microns and the rest of the thickness is Zry-4 to provide the mechanical strength.
[6] All AREVA duplex claddings contains Zry-4 with 1.5 wt%Sn
[7] Zry-4 with 1.3 wt %Sn
[8] Zry-4 with 1.5 %Sn
[9] Zry-4 with 1.5%Sn

3 Impact of irradiation on fuel performance

3.1 Introduction

During irradiation, the thermal, mechanical and chemical conditions in a fuel rod vary with power, exposure or time and operating history. The temperature of the fuel follows a nearly parabolic distribution across the pellet radius and varies strongly with power. It also varies with the thermal conductance of the pellet-to-cladding gap, the cladding itself, the oxide, *CRUD* and water films on the outside surface of the cladding and with the bulk coolant temperature. Inside the fuel rod, several processes occur during irradiation, as follows.

Early life is characterized by transfer of heat across the gas-filled gap between pellets and cladding, which almost universally contains helium. Early life also involves a number of processes that affect thermal and structural conditions in the rod; e.g.:

- Fracture of the fuel pellets due to thermal stresses starting on the first rise to power and continuing during the initial 5 – 10 GWd/MTU according to power and power history.
- Relocation of the resulting fuel fragments toward the inner cladding surface.
- Pellet densification, which is typically small in modern fuel.
- Depending on the pellet manufacturing process, the evolution of a small amount of volatiles.

On the inside of a fuel rod, continued irradiation leads to:

- *FGR* with increasing gas pressure inside the fuel rod and decreasing thermal conductivity of the helium filler gas due to the addition of krypton and xenon.
- Solid and gaseous swelling due to the accumulation of fission products and the formation of bubbles and other gas filled voids.
- Inward cladding creep due to the temperature, fast neutron flux and the net difference between internal gas and external coolant pressures.
- Increasing amounts of pellet-cladding mechanical interaction due to gap closure by relocation, swelling, cladding creep down and differential thermal expansion between pellets and cladding.
- Healing of the cracks among pellet fragments by in situ sintering to a degree that depends on operating conditions and history.
- Hot pressing and the formation of dishes on the ends of flat pellets or filling of dishes, which were formed during pellet fabrication.
- The release of fission products with the potential for contributing to cladding failure by processes such as Stress Corrosion Cracking (*SCC*) or liquid metal embrittlement; i.e., iodine or cadmium with caesium.

At moderate to high exposures, the chemistry of the fuel changes in a manner, which can affect its thermal and mechanical properties. An example is an increase in the pellet oxygen-to-metal ratio leading to a decrease in thermal conductivity, an increasing pellet temperature and an increase in pellet creep rate. With sufficient contact at the pellet-cladding interface, temperature and time, oxygen can also be transferred from the fuel pellets to the cladding (fuel-clad bonding).

On the outer surface of a fuel rod, exposure, time, temperature or combinations of these factors lead to oxidation of the cladding and deposition of corrosion products *CRUD* from reactor internals and piping. Surface corrosion reduces the thickness of the cladding wall and leads to the pickup of hydrogen in the cladding metal. Wall thinning is typically small in modern zirconium-based cladding, but is addressed in the design process and is identified as a key factor in postulated *LOCA*s. Hydrogen pickup leads to concentrations in the cladding that increase with exposure or time and normally exceed the solubility limit at operating temperatures by low-to-moderate burnups. Hydrogen concentrations in excess of the solubility limit lead the precipitation of hydrides. Such hydrides are brittle relative to zirconium-based cladding. At sufficiently large concentrations, hydrides can degrade the strength and ductility of the cladding. The density of zirconium hydride is lower than that of zirconium, so that their precipitation generates local strains in the cladding. With increasing concentrations, the combination of low ductility and local strains can cause structural failure at the location of hydride blisters, lenses or sunbursts. Based on experience in Japanese power and test reactors, hydrides have also been implicated in an outside-in, hydride-assisted fuel cladding cracking process.

The different processes going on in the fuel rod are interrelated in a highly non-linear manner. They are shown schematically in Figure 3-1 and Figure 3-2.

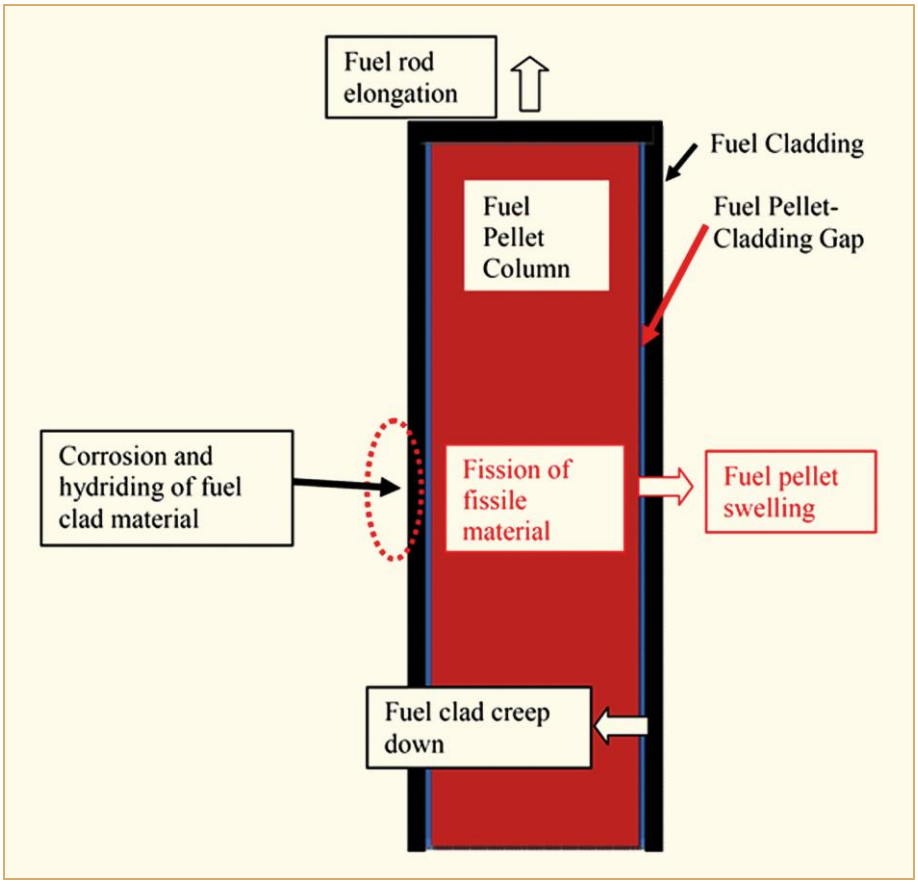

Figure 3-1: Schematic showing the different processes occurring in the fuel rod during irradiation.

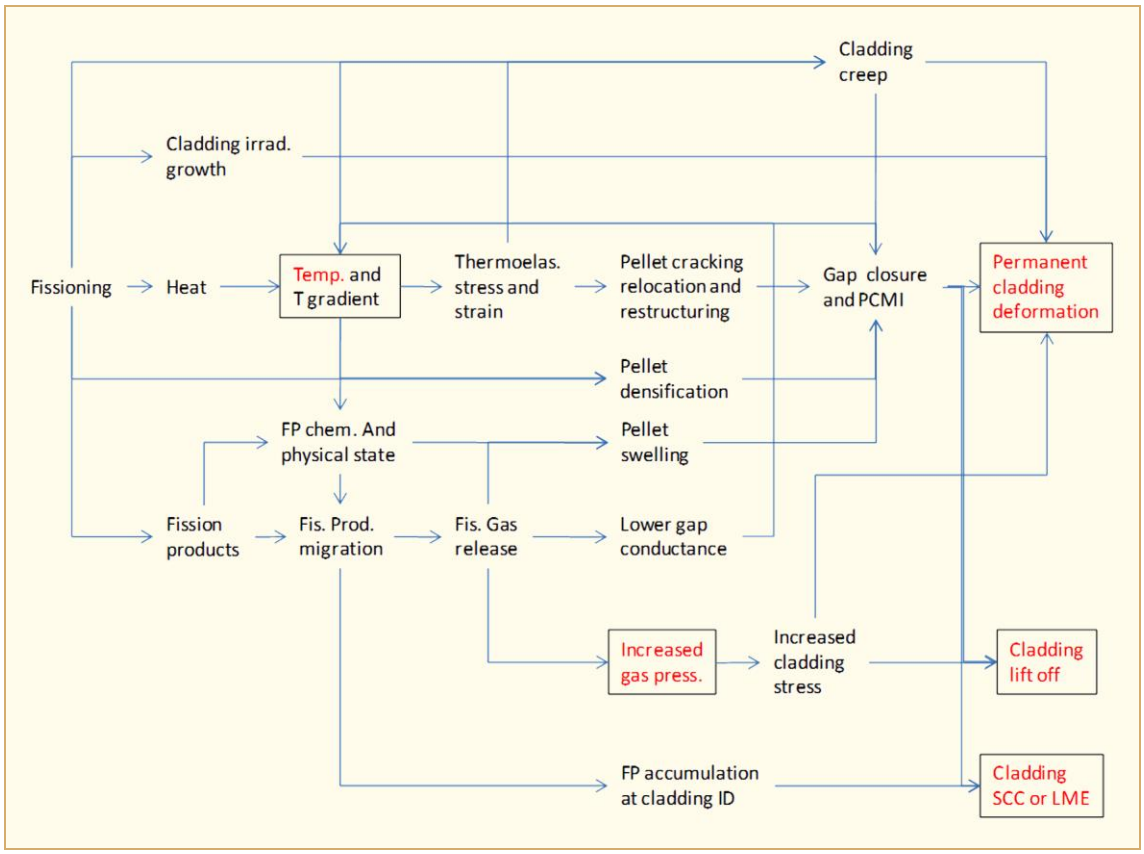

Figure 3-2: Schematic diagram of the principal internal, fuel rod processes and their primary interactions. (Key design criteria are enclosed with a box and shown in red).

3.2 Fuel pellet

When fission takes place in the fuel pellet, the excited compound nucleus formed after absorption of a neutron breaks up into two lighter nuclei, called fission fragments. Three nuclides, having sufficient stability to survive for a long time, namely, ^{233}U, ^{235}U, and ^{239}Pu, are fissionable by neutrons of all energies. Of these nuclides, ^{235}U is the only one that occurs in nature. During the irradiation, ^{235}U is being consumed while the fissionable materials ^{239}Pu and ^{241}Pu are being produced by epithermal neutrons, especially at the fuel pellet periphery. The fissioning and capture processes are biased toward the pellet periphery because of self-shielding by ^{235}U and ^{239}Pu and by the high cross section fission products. This bias varies during the course of irradiation due to changes in the fuel pellet and, in *BWR*s, due to changes in the neutron spectrum associated with variations in the local coolant void fraction.

The energy yield from fissioning varies slightly among reactor types and fuel design, but is in the range of ~200 MeV/f. As a useful reference, fissioning of 1 gram of material per day produces approximately 1 megawatt of power. The majority of the fission energy, >80%, is in the form of kinetic energy of the fission fragments, which appears immediately as heat. The remaining energy is distributed among instantaneous gamma rays from excited fission fragments, kinetic energy of fission neutrons, beta particles and gamma rays from fission products and neutrinos. The energy of all except the neutrinos ultimately appears as heat. Essentially all of the neutrinos and accompanying beta particles escape due to their weak interaction with materials in a fission reactor.

About 200 stable or long-lived fission product atoms are produced within the fuel per 100 fissions. The mass numbers of most of the fission products (~94%) range from 95 to 139 and exhibit a bimodal distribution, with a "light" group centred at ~85 and a "heavy" group at ~140. Most of the fission products are radioactive and decay by the loss of a negative beta particle. So, the initial radionuclides transmute into ~200 fission products. These fission products fall into 5 groups based on their physical or chemical state and on their solubility in the fluorite (UO_2) matrix; viz.:

1) Soluble oxides such as the rare-earth fission products, some molybdenum, niobium, yttrium, some zirconium and the transuranics.
2) Insoluble oxides such as barium, strontium, and the remaining zirconium in the form of zirconates (e.g., $BaZrO_3$ and $SrZrO_3$).
3) Metallic precipitates such as some rhodium, ruthenium, technecium and the remaining molybdenum.
4) Fission products with low melting temperatures and high vapour pressures (volatiles) such as caesium, iodine, tellurium, rubidium that can exist as either a gas or a solid depending on their location inside a fuel rod.
5) Gases such helium, krypton and xenon.

The chemical state of molybdenum depends on the local temperature and oxygen potential of the fuel. Molybdenum functions as a buffer for oxygen and tends to stabilize the oxygen-to-metal ratio. If the oxygen potential can be estimated (as in nearly stoichiometric UO_2 at low-to-moderate burnup), the pellet radius for the transition from Mo to MoO_2 is sometimes used with related thermal calculations as a loose check of fuel temperature and power.

The combined production rate of long-lived and stable Xe and Kr is 0.25 atoms per fission (Meek & Rider, 1974), which corresponds to about 30 ml of gas at Standard Temperature and Pressure (*STP*) per 1 MWd/kgU burnup for each kilogram of fuel. The production rate varies slightly depending on the relative amounts of heat generation due directly to fissioning and due to energy conversion outside of the fuel rod and depending on the relative fissioning rates of uranium and converted-in plutonium (burnup).

The irradiation impacts the following fuel pellet characteristics:

- *Pellet density* - At low burnups a densification can be observed (seen as a negative swelling rate) depending on the type of fuel (porosity, pore size, and grain size). At burnups up to about 50 MWd/kgU the swelling rate is in the range of 0.4 – 0.8 $\Delta V/V$ per 10 MWd/kgU, due to UO_2 solid swelling and swelling by formation of fission gas bubbles in the hot centre of the fuel pellet. At higher burnups, the swelling rate increases to about 1.5% $\Delta V/V$ per 10 MWd/kgU due to the formation of the porous high burnup rim. Density also varies with pellet-to-cladding mechanical interaction. That is, the mechanical restraint of the fuel cladding induces compressive stresses in fuel pellets. The hydrostatic component of these stresses leads to hot pressing and closure of pellet porosity. The hydrostatic component also combines with UO_2 surface tension to support the pressure of fission gas in bubbles and other closed voids.
- *The fuel melting point* – The fuel melting temperature is a design limit for the maximum allowable *LHGR* during a Class II power transient. The melting temperature decreases slightly with exposure, due primarily to the accumulation of conversion and fission products and due to increasing oxygen potential.
- *Burnup* - At pellet average burnups in excess of about 50 MWd/kgU a particular structure is formed at the rim of the UO_2 pellet. The transformed zone is usually called *high burnup rim zone*. Formation of this High Burnup Structure (*HBS*) is characterized by (or results from) a simultaneous formation of a sub-grain structure leading to an amorphous appearance, an increase in porosity and the transfer of fission gas from the *HBS* UO_2 matrix to the pores. The rim structure is a feature of ongoing research relative to high burnup and transient behaviour. It affects the thermal conductivity and is postulated to increase *FGR* during a *RIA* and *LOCA* due to fragmentation of the rim zone under the excessive overpressure in the pores.

- *Thermal conductivity* – The thermal conductivity of UO_2 is a key parameter in fuel performance and in code calculations since conductivity impacts important properties such as fuel temperature, thermal expansion, *FGR* and gaseous swelling. Most of the thermal conductivity values are calculated from thermal diffusivity values measured by laser flash methods. Thermal conductivity is the product of thermal diffusivity, heat capacity, and density.

  Thermal conduction in UO_2 is a complex physical process and depends on many parameters such as the temperature, the density (porosity), the stoichiometry (the U/O ratio), impurities, additives, and the duration of irradiation (burnup) as follows,:

  Eq. 3-1 $$\lambda = \kappa_1(\beta)\kappa_2(\rho)\kappa_3(x)\kappa_4(r)\lambda_0(T)$$

  $\kappa_1(\beta)$ = burnup dependence factor
  $\kappa_2(\rho)$ = porosity/bubbles contribution
  $\kappa_3(x)$ = effect of U/O relative to burnup
  $\kappa_4(r)$ = radiation damage
  $\lambda_0(T)$ = thermal conductivity of unirradiated fuel

  As noted above, the specific heat capacity and thermal conductivity of UO_2 are inter-related by way of density and thermal diffusivity. Heat capacity is a principal factor in the energy stored within a fuel rod and must be considered in *LOCA*, *RIA* and other transient analyses. Thermal conductivity, density and heat capacity decrease with burnup and are addressed in most thermal-mechanical models that are structured for evaluations of fuel performance at moderate-to-high burnup.
- *FGR* - A significant fraction of the fission gases Xe and Kr are located in the UO_2 lattice at low temperatures (<1200°C). Another fraction of the fission gases is located in the small intragranular and the larger intergranular pores. A third fraction is released to the plenum. *FGR* is usually divided into thermal[10] and athermal[11] release mechanisms based on the role of thermally activated processes on gas release.

  Athermal FGR takes place at all fuel temperatures and burnups by recoil and knockout of fission gas atoms by energetic fission fragments. Since only fission gas atoms located within a short distance of the fuel surface (≈10 μm) can be released by this mechanism, the contribution of this *FGR* mechanism is small (much less than 1% of the fission gases produced), but increases with operationally dependent increases in the specific surface area (surface-to-mass or volume ratio) of the fuel pellets.

  Thermal FGR only occurs if the fuel temperature and the burnup are large enough to activate temperature-based processes such as diffusion and grain growth. The thermal component of *FGR* can potentially result in large release fractions even at moderate burnups.

[10] Temperature dependent
[11] Temperature independent

Thermal release mechanism consists of three processes:

1) Diffusion of fission gas atoms from the grain interior to the grain boundaries, sweeping of gas atoms by growing grain boundaries or combinations of these factors.
2) The formation, growth and coalescence of gas bubbles at the grain boundaries.
3) The interlinkage of grain boundary gas bubbles forming channels at the grain boundaries connected to the fuel rod void. This results in the release of the gas stored on the interlinked grain boundary porosity and in a dramatic shortening of the diffusion distance of the fission gas atoms from grain interior to open voidage (gap and plenum volume). The consequence is a dramatic increase in the *FGR* to the fuel rod plenum and a sustained increase in the release rate. Thermally activated gas release can lead to a large increase in fuel rod internal gas pressure, a decrease in the thermal conductance of the pellet-cladding gap, higher pellet temperatures and more gas release.

Vitanza et al., 1979, proposed an empirical 1 % *FGR*[12] threshold curve for UO_2 fuel, based on a large set of data. The general dependence of this threshold on pellet temperature and time agrees well with both on-line measurements of surface-to-volume ratios and post-irradiation observations of interlinkage. Today, it is observed that the original Vitanza curve overestimates the temperature at which 1 % *FGR* occurs at high burnups, Wiesenack, 2003. In Figure 3-3 the empirical Vitanza threshold is shown together with more recent code calculations of this threshold and recent experimental data at higher burnups. The figure shows that the fuel temperature (related to the *LHGR*), where thermal *FGR* starts (indicated by the 1% *FGR* lines), decreases with burnup. At burnups >80 MWd/kgU the fractional *FGR* reaches values >15% even at low *LHGR* values (≤200 W/cm).

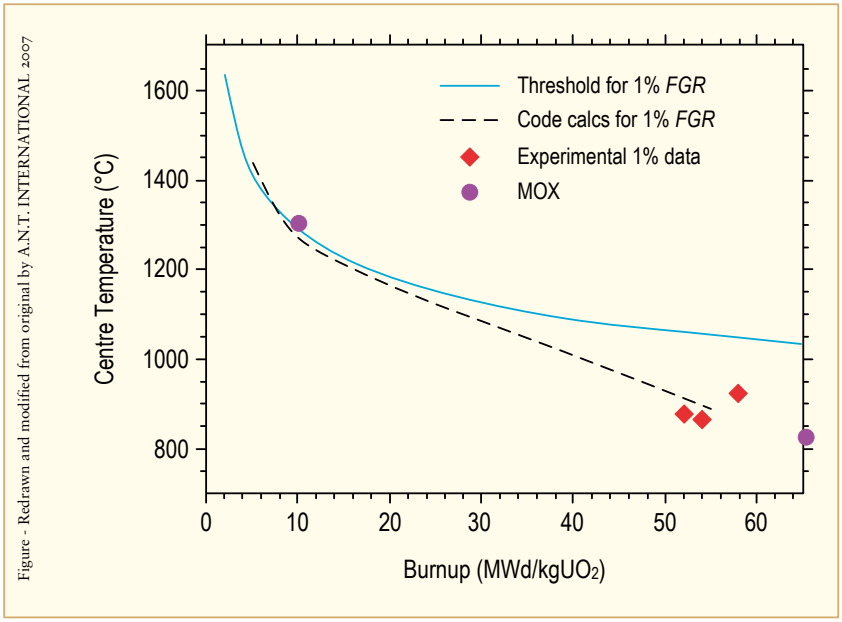

Figure 3-3: Empirically derived correlation for >1% (thermal) *FGR*, Vitanza et al., 1979, code calculations and recent experimental data, Wiesenack, 2003.

[12] i.e. 1% of the total amount of fission gases are released to the fuel-pellet gaps and plenum in the fuel rod. The region above the 1 % curve represent temperature-burnups where thermal *FGR* dominates while the region below this curve correspond to temperature-burnups where athermal *FGR* mechanisms dominate.

Figure 3-4 and Figure 3-5 shows increased *FGR* increases the rod internal pressure and reduces the margins towards *liftoff*.

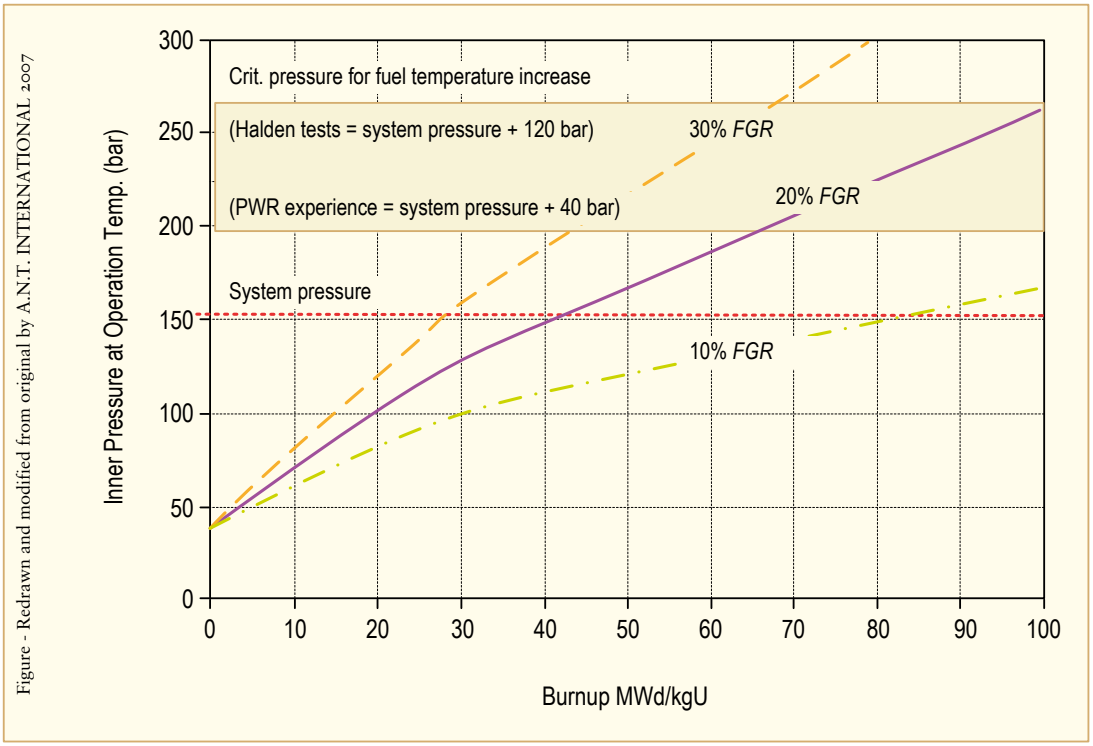

Figure 3-4: Calculated inner pressure for 17*17-fuel rods with a length of 3848 mm, an active length of 3658 mm, a 9.5*0.57 mm cladding, a pellet diameter of 8.19 mm, a UO_2-density of 10.43g/cm³, and a pre-pressure of 20 bar.

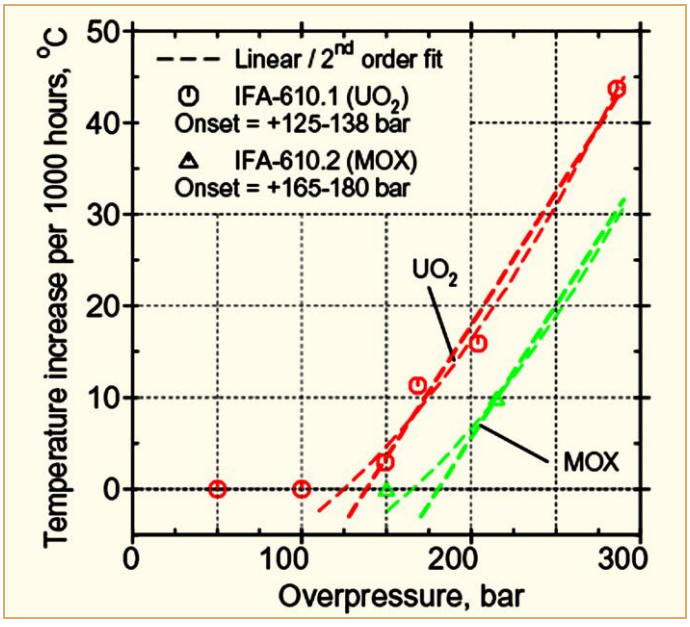

Figure 3-5: Summary of the Halden data on the response to overpressure. The intercept of the dashed curves with the 0 "Temperature increase" indicates onset of *liftoff* (re-opening of the fuel-pellet gap resulting in a fuel pellet temperature increase) Wiesenack, 2003.

The Transient Fission Gas Release (*TFGR*) during and after a power ramp is also an area of interest. The *TFGR* value depends on ramp terminal power, the holding time at ramp terminal power, the burnup, the fuel microstructure (e.g., grain size, porosity, etc.) and pellet-cladding mechanical interaction. The *TFGR* will increase the *PCI*/Pellet Cladding Mechanical Interaction (*PCMI*) loading during a power transient. Increased *PCMI* can lead to increased hydrostatic stress in the fuel pellets, which affects the rate of gaseous swelling as well as the onset of gas bubble interlinkage and the *FGR*. The nature of such changes depends on a balance of forces due to gas bubble pressure, UO_2 surface tension and elastic, plastic and creep deformation of the pellets and cladding. These processes depend on the operating history of the fuel and are difficult to relate to a specific behaviour. For reference, however, operation involving an extended interval at low pellet temperature with little or no porosity interlinkage is expected to give larger increments of gaseous swelling on a ramp to high temperatures than operation at temperatures corresponding to the upper bound of commercial *LWR* fuel or with frequent cycling to such temperatures. In the former (low-high power) case, gas release can be delayed until the power decrease following the transient by hydrostatic stress in the fuel pellets. With the pellet restructuring that takes place during or after the transient, gas release is strongly dependent on the transient temperature and time.

3.3 Zr alloy materials

3.3.1 Irradiation damage

The irradiation of neutrons with energies in excess of about 40 eV will result in damage of the zirconium alloy lattice. The higher energy of the neutron and the lager the fluence, the larger lattice damage. This damage will change the zirconium alloy properties dramatically. Such changes include:

- An increase of yield and ultimate tensile strength.
- A decrease of ductility.
- An increase in corrosion rate (NB: The decomposition of the water by neutron interactions and other irradiation effects will also increase the corrosion rate by itself).
- An increase in rate of dimensional changes due to increases in:
  - Creep rate (also including residual stress relaxation).
  - Irradiation growth and growth rate.

In structural materials like zirconium alloys, the overwhelming majority of defects are caused by the collision of neutrons with lattice atoms. These collisions produce vacancies and interstitials. Some of the interstitials recombine with vacancies. Others are absorbed by dislocations, which are then able to climb and concentrate between crystal planes. The remaining vacancies condense in crystal planes. Collapse of the affected lattice leads to the formation of self-interstitial and vacancy loops. They are collectively called prismatic loops and differ from loops formed by shear along a glide plane. Interstitial and vacancy loops form on prism planes and are identified by the normal to the prism plane; i.e., an <a> loop. Vacancy loops form on basal planes and are also identified by the normal to the basal plane; i.e., a <c> loop. <a> loops form relatively early in the irradiation. Their number density saturates asymptotically with increasing neutron fluence. The increase in *<a> loop density increases the strength and lowers the ductility and fracture toughness of the Zr alloy material. Thus, the strength increase and ductility/ fracture toughness decrease due to this effect typically reach ~90% of their respective long-term values between 5 and 10 MWd/kgU. The ductility/fracture toughness of the Zirconium alloy may however continue to decrease with burnup due to the hydrogen pickup occurring during the corrosion reaction between the water molecule and the Zr alloy material.*

The <c> type of loop induced by radiation does not form until later in life. In Recrystallised Annealed (*RXA*) Zircaloy-2 and -4, <c> loops are first observed at a burnup of around 15 MWd/kg and increase in density during the rest of the fuel lifetime. In Stress Relieved Annealed (*SRA*) Zircaloys, <c> type dislocations remain from fabrication and will result in <c> type loop formation already at start of irradiation. *<c> loops are thought to strongly influence irradiation growth and creep behaviour, but probably do not affect mechanical properties. The lower irradiation growth rates of M5 and ZIRLO appear to be due to the difficulty in forming <c> loops in these alloys.*

The formation of point defects such as interstitials and vacancies during irradiation will also change the creep mechanism from that during out-of-reactor conditions. The consequence is that the creep resistance ranking between different materials may be different out-of-reactor compared to in-reactor. As an example, the creep rate is larger for *SRA* than for *RXA* Zr alloy materials in-reactor while the reverse ranking is true for out-of-reactor. *This means that one should be cautious in interpreting out-of-reactor creep test results for in-reactor conditions.*

Corrosion resistance in zirconium alloys is intimately related to the protective part of the ZrO_2 layer (often called barrier layer) which in turn is partly related to the presence of SPPs formed in the zirconium matrix by deliberate additions of alloying elements and by heat treatments to control their size. In as-fabricated Zircaloy-4 the most common *SPP* is $Zr(Fe, Cr)_2$, while in Zircaloy-2 they are $Zr(Fe,Cr)_2$ and $Zr_2(Fe, Ni)$. For the ZrNb type alloys (such as M5) the most common is βNb (which is not an intermetallic). For the ZrSnNbFe alloy types (such as *ZIRLO*, *MDA* and *NDA*) the most common types are $Zr(Nb,Fe)_2$ and βNb. At normal *LWR* temperatures (270-370°C (543-643K)) the *SPP*s change under irradiation in a combination of two ways – amorphization and dissolution.

Amorphization means that the original *SPP* crystalline structure is converted to an amorphous structure. A critical temperature exists above which the annealing processes are fast enough to prevent the accumulation of defects needed to transform crystalline *SPP*s to amorphous structures. For typical reactor irradiations, amorphization of both $Zr(FeCr)_2$ and $Zr_2(Fe,Ni)$ in Zry-2 occurs readily at temperatures near 100°C (373K). But, at the temperatures (300°C(573K)) and neutron flux encountered in a *LWR*, $Zr(Fe,Cr)_2$ becomes amorphous but $Zr_2(Fe,Ni)$ does not. Above about 330°C (603K), neither *SPP* becomes amorphous.

The fluence required to produce complete amorphization depends on neutron flux, temperature and *SPP* size and chemistry. But, for typical $Zr(Fe,Cr)_2$ *SPP*s of initial size near 0.1 μm, the entire *SPP* is amorphous by end of bundle life burnups, <50 MWd/KgU ($1x10^{26}$ n/m², E>1 MeV). *The rate of dissolution depends on the SPP size, with higher rates for smaller sizes. The extent of dissolution depends on size and fluence.* It has been demonstrated in a *BWR* that small (<0.04 μm) *SPP*s in Zry-2 can completely dissolve at low to moderate burnups. Also in a *PWR*, but at temperature near 290°C, *SPP*s in Zry-4 with an average size of 0.2 μm were >80% dissolved at moderate burnup (1×10^{26} n/m², E > 1MeV). ***The consequence of the complete dissolution of the SPPs in Zry-2 and Zry-4 is a dramatic increase in the Hydrogen PickUp Fraction (HPUF) and, after some time, also an acceleration of the corrosion rate in BWRs.***

For the Zr-Nb type alloys preferentially used in PWRs neither the βNb nor Zr (Nb, Fe)₂ SPPs become amorphous (or dissolve) for irradiation temperature >330°C (603K).

SPP amorphization in itself does not appear to affect material behaviour; however, dissolution of both amorphous and crystalline SPPs does influence corrosion and growth.

In the following subsections, more details are given on how the neutron damage changes the zirconium alloy microstructure, which in turn changes the properties of the Zr alloy material.

3.3.2 Corrosion

Corrosion of zirconium alloys is a thermodynamic and electrochemically based process affected by the following parameters, see Figure 3-6:

- Protectiveness of the zirconium oxide film formed which depends on:
  - The microstructure of the metal surface.
  - The water chemistry and the hydraulic conditions.
- The Zr alloy temperature (at the metal/oxide interface).

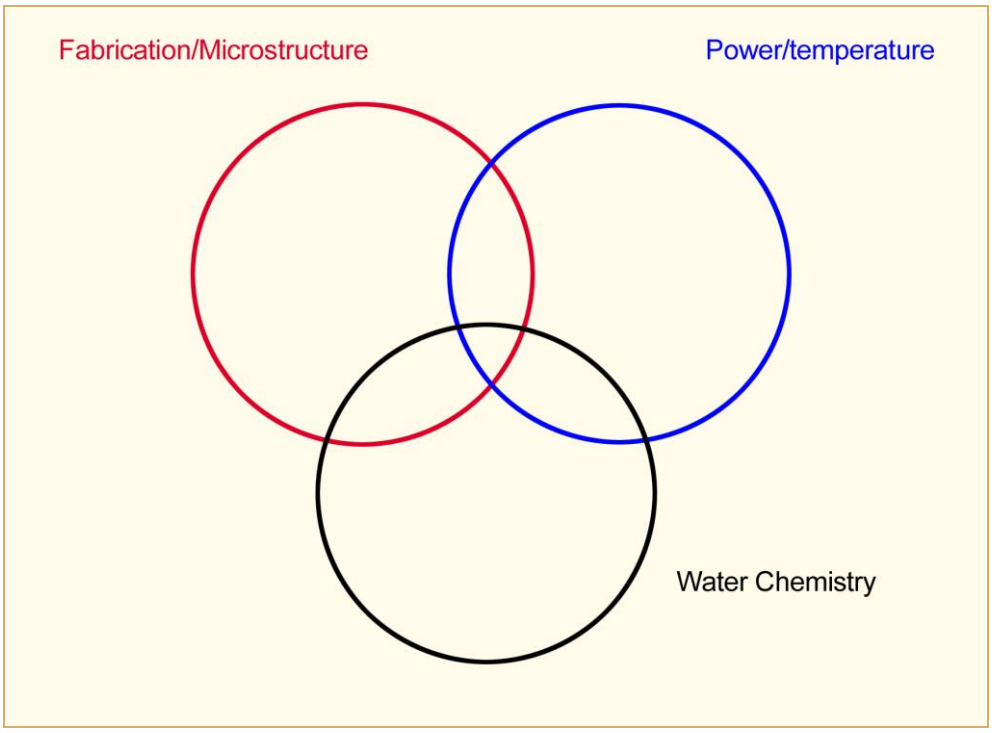

Figure 3-6: Parameters impacting corrosion performance of Zr Alloys.

Irradiation affects the metal microstructure, the oxide properties and the water chemistry. Since the corrosion mechanisms are different in out-of-reactor corrosion (autoclave) tests and in-reactor operation, *the oxide thickness and hydrogen pickup estimations by the fuel vendor must be based upon or somehow normalized to in-reactor data.*

In *BWR*s there are different types of corrosion modes:

- Nodular corrosion starting after 10 to 100 days of irradiation in material with large *SPP*s, Figure 3-7 and Figure 3-9
- Shadow corrosion starting after a few days of irradiation, Figure 3-8 and Figure 3-9
- Uniform corrosion that starts at the beginning of irradiation at a rapid rate, slows quickly and then increases later in life by changes in the nature of the oxide layer, Figure 3-7 and Figure 3-9

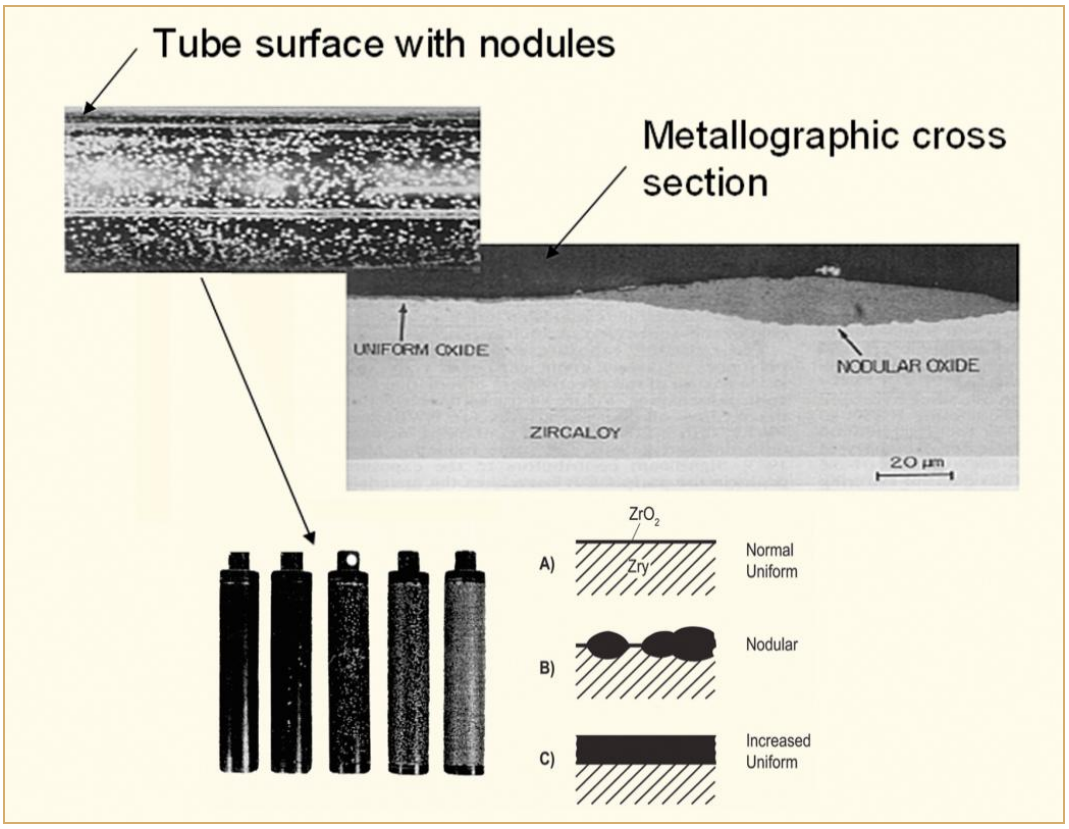

Figure 3-7: Corrosion morphology for Zircaloy, Adamson et al., 2007/2008.

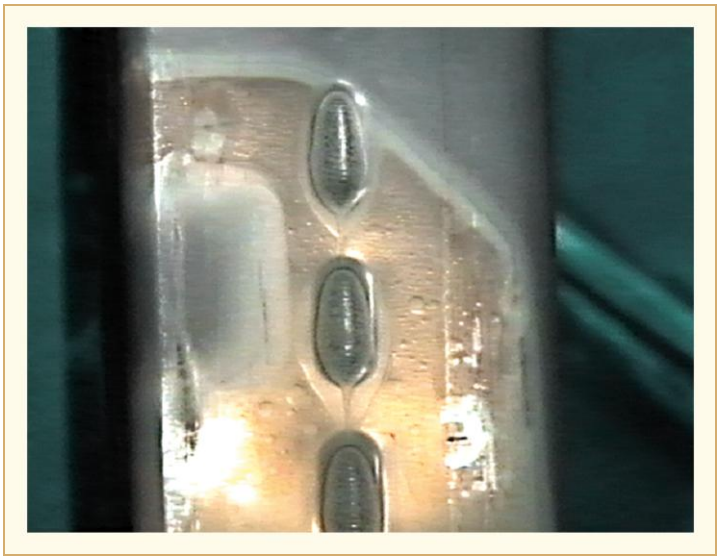

Figure 3-8: *BWR* channel control rod handle shadow corrosion.

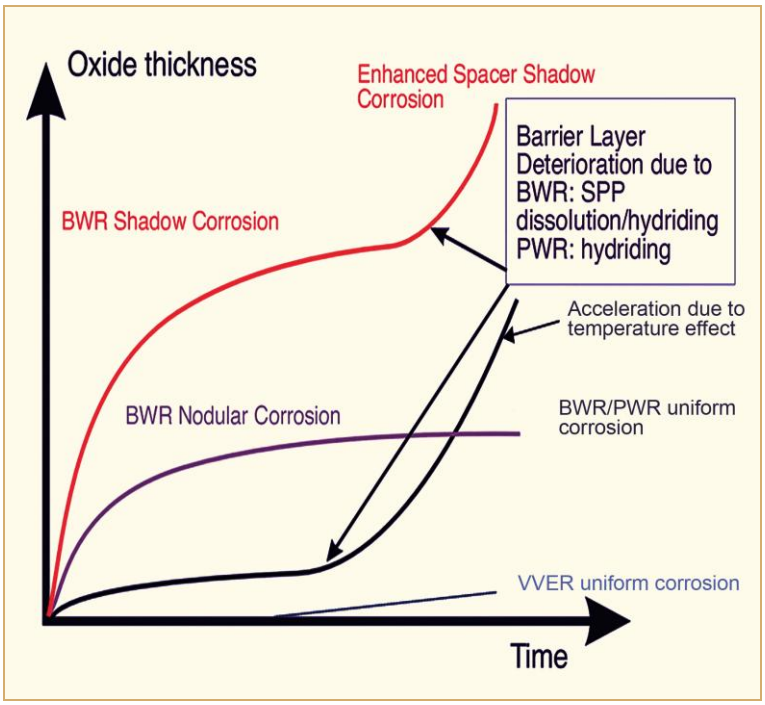

Figure 3-9: Oxide growth shown schematically in *BWR*s, *PWR*s and *VVER*s.

Depending on the *BWR* Zr alloy microstructure, the alloy may show either uniform or nodular corrosion or a mix of both. There is an increase of tendency for nodular corrosion if the Second Phase Particle (*SPP*s), in the Zry-2 material are large in size; i.e. greater than about 0.15 µm. Large *SPP*s and excessive nodular corrosion were contributing factors in the rash of *CRUD* Induced Localised Corrosion (*CILC*), fuel failures that occurred in the 1970s[13]. As a result, fuel vendors modified the fuel cladding composition and manufacturing process to reduce the *SPP* sizes in the 1980s. These changes as well as changing the coolant water chemistry resolved this issue. Smaller *SPP*s tend to favour uniform corrosion. However, during irradiation there is a tendency for the *SPP*s to dissolve, with smaller *SPP*s dissolving at a faster rate than larger *SPP*s. At a certain point, the *SPP*s become so small they are not longer able to form a protective barrier layer. Below a limiting size, the rates of oxidation and hydrogen pickup have been observed to increase at higher burnups. The need to reach higher burnups without getting increased corrosion rate and *HPUF* late in life (due to *SPP* dissolution) have prompted some fuel vendors to modify the cladding tube manufacturing process again by increasing the *SPP* size distribution somewhat (but still lower than that size which may result in nodular corrosion). *SPP* sizes greater than ~0.08 µm are reported to give the lowest corrosion rates in both *BWR*s and *PWR*s, Figure 3-10.

[13] Also, power history and water chemistry were important parameters resulting in the *CILC* failures. It was noted that $(U,Gd)O_2$ rods showed a much larger tendency for nodular corrosion and *CILC* failures compared to sibling UO_2 rods. This difference was attributed in part to the low power early in the life of $(U,Gd)O_2$ rods. The fuel rods that failed due to *CILC* were also covered with a *CRUD* layer containing large amounts of copper in addition to the iron. The large fraction of copper in the *CRUD* originated from aluminium brass condenser tubes and filter demineraliser cleanup systems. Most plants with aluminium brass condensers replaced them with other materials; e.g., titanium. Today only a few plants operate with aluminium brass condensers.

4 Fuel vendor licensing data

To ensure the safe performance of fuel assemblies and reactors, certain design, operating and licensing criteria are specified. These criteria are discussed in detail in *FMTR* Vol. 2 and in a survey of Nuclear Energy Agency (*NEA*) countries which was conducted by the CSNI Special Expert Group on Fuel Safety Margins, *NEA*/CSNI/R(2003)10. For reference, the relationship among these criteria are shown schematically in Figure 4-1 The safety criteria, summarized in Table 4-1 are typically imposed by regulators based on technical risk as determined by theoretical analyses, experimental data, operational experience or combinations of such information. Many of these limits relate to accident and transient conditions. The safety limits must be met at all times and constitute the primary basis for the operating and design limits. The operating limits, summarized in Figure 4-1, cover normal operation and operational occurrences that are expected to be more frequent than the accidents and transients comprising the safety limits. As shown in Figure 4-1, operating limits are reduced relative to the corresponding safety limits by margins that reflect uncertainty in the underlying data, analytic methods and operational measurements. Many of the operating limits are unique to a specific fuel design. They are typically provided by the fuel supplier and approved by the regulators as part of the licensing processes. The design limits, summarized in Table 4-1, constitute the technical bases for the fuel and are structured to assure compliance with the safety and operating limits. As in the relationships between the safety and operating limits, the design criteria include safety margins relative to the corresponding operating limits. Design criteria are specified by the fuel suppliers and are usually proprietary to the supplier. Some design criteria are explicitly approved by the cognisant regulator, while others are implicitly approved by way of their effects on related safety and operating criteria. Other design criteria are also specified by the fuel supplier independent of the regulatory limits to assure economic and reliable performance.

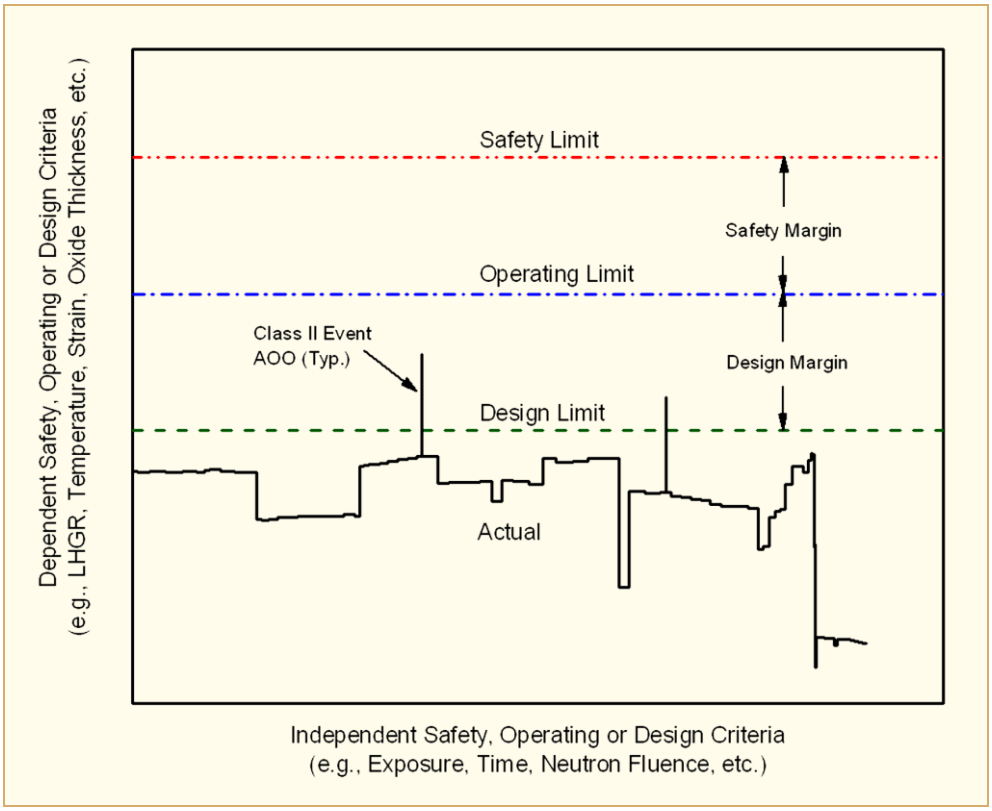

Figure 4-1: Schematic relationship among design, operating and safety criteria.

Table 4-1: Summary of safety criteria [after *NEA*/CSNI/R(2003)10], *NEA*/CSNI/R(2003)10.

Limit	Criteria	Basis	Notes
Critical Heat Flux (*CHF*), *DNB* or CPR	Various, depending on country, correlation and reactor type	Empirical correlations with statistical treatment of uncertainties	Values dependent on design
Reactivity coefficient	Overall negative reactivity	Prompt inherent feedback	Rational varies among countries; i.e., conservative best estimate, statistical
Shutdown margin	Boron, control rod worth	Attain subcriticality	Varies with country, reactor and core design
Enrichment	No explicit limit in most countries, but almost universally restricted to ≤5% ^{235}U	Transportation, manufacturing and storage limits	The enrichment limit is a topic of ongoing deliberations but shows no signs of increasing at this time.
Internal gas pressure	Pressure or cladding lift-off depending on the country	$P_{gas} < P_{sys}$ or no increase in pellet cladding gap due to gas pressure	The gas pressure limit is generally applied in a conservative manner based partially on deterministic and partially on statistical methods.
PCMI	Varies among countries; i.e., strain, stress, maximum power increase or no explicit limit	• Hoop stress < SF*Yield Stress • ≤1% elastic + plastic strain • ≤2.5% equiv. plastic strain • Demonstrate low probability of *PCMI* failure based on ramp tests	The 1% limit on elastic + plastic strain appears to be the most common criteria. It is usually applied on a conservative basis.
RIA fragmentation	Increase in radially-averaged fuel enthalpy (common) or no fuel melting (less common)	Experimentally based with different limiting values among countries and, in some cases, with exposure	Topic of active investigation and change due to the introduction of new cladding alloys and operation to higher burnups
Non-*LOCA* runaway oxidation	Either no limit or a bound on cladding temperature	Experimentally based where applied, with value in the range of 1220 - 1480°C	
LOCA Peak Cladding Temperature (*PCT*)	Temperature ≤1200 or 1204°C (≤1760°C in Canada)	Experimental determination of oxidation and embrittlement	Conservative models and assumptions widely used for licensing; more realistic, best-estimate models available for estimation of design margin
LOCA Cladding Oxidation	Equivalent Cladding Reacted (*ECR*) ≤17% (18% for *VVER* 440)	Experimental determination of oxidation and embrittlement	Criteria under revision in US and other countries due to new cladding alloys, operation to higher burnups and the recognition of additional processes that affect post-quench ductility
LOCA hydrogen release	H release ≤ 1% of the theoretical amount generated if all of the cladding in the active core reacted	• Related to *LOCA* oxidation • Intended to assure containment integrity	
LOCA long-term cooling	• Long-term stability after accident • Decay heat removal	Qualitative	
Seismic loads	Acceleration or force limits where seismic criteria are imposed	• Control rod insertability • Core coolability • Deformation limits	
Hold-down forces	Qualitative limit	Prevent lift-off of *FA* by hydraulic forces in Class I and II events	
Criticality	Margin to criticality ≥ 2 or 5% based on moderation	Avoid criticality during fabrication, transportation or storage	Burnup adjustments allowed in some countries
Burnup	Varies among countries, reactor types and fuel designs; e.g., limit on average assembly(45-60 GWd/MTU), average rod (58 - 65 GWd/MTU)or peak pellet (55 - 75 GWd/MTU) and type of fuel (UO_2 or Mixed OXide (*MOX*))		

Table 4-1: Summary of safety criteria [after *NEA*/CSNI/R(2003)10], *NEA*/CSNI/R(2003)10 (Cont'd).

Limit	Criteria	Basis	Notes
CHF, *DNB* or CPR	Varies with country and, in some cases, with plant and fuel; Values in range of 1.2 - 1.8	*CHF*, *DNB* or CPR safety limits with model and measurement margins	Typically conservative, but also statistically based in many cases
LHGR	*LHGR* versus burnup curve that typically varies by country, plant and fuel	Steady state margin to safety limits, including Class II events (*AOO*s) for key characteristics such as • Fuel melting, • Rod internal pressure, *FGR* • Cladding strain, stress and fatigue	Limiting *LHGR* curve(s) constructed analytically using models validated relative to in-core experience
PCI	Varies among countries from no limit to rules on power changes, conditioning and deconditioning	Generally based on ramp test experience where limits are imposed	The absence of a *PCI* criteria is typically based on the limited extent of such failures and a position that they pose economic rather than safety issues
Coolant and/or offgas activity	Varies with country and plant	Limit release after fuel failure	
Source term activity	Varies with country	Limit release after larger scale fuel failure	
Control rod drop or insertion time	Varies with country and plant	Assure safe shutdown	
RIA fuel failure limit	Enthalpy rise that varies with country, reactor type and, in many cases, with burnup	Margin to *RIA* fuel dispersal limit	Area of active review due to the introduction of new cladding materials and operation to higher burnups

5 Root cause examinations of failed and degraded fuel

5.1 Introduction

For political and economical reasons, there are objectives to reduce the primary fuel failure frequency as much as possible and to minimize the consequences of fuel failures when they occur.

Fuel failures can have adverse impact on:

- Power generation.
- Outage time.
- Chemistry and radiation monitoring costs.
- Personnel exposure.
- Handling, transportation and storage or reprocessing.

The cost per failure was recently estimated by Lemons, 2008 to range from $1 000 000 to more than $20 000 000 depending upon the type of reactor, the need for power suppression or a mid-cycle outage, reduced cycle length, the cost of replacement energy and the impact of the leaking fuel on subsequent core designs, operation and post-irradiation handling. The loss of generating capacity is a significant component in the cost of fuel failure. Generating capacity can be lost in power suppression tests to locate leaking fuel assemblies, in power reductions to minimize the risk of degradation of a leaking fuel rod, in mid-cycle outages to remove leaking assemblies and in operating cycles that are cut short by control blade insertions or unacceptably high coolant or off-gas activity. Generating capacity can also be adversely affected in subsequent reactor cycles by non-optimal core loading or operating compromises as a result of action taken to manage a leaking *FA*.

While both *BWR*s and *PWR*s are capable of operating with leaking fuel rods without adversely affecting safety, degradation of the affected rods after failure (secondary damage or degradation) can increase the release rate of gaseous, soluble and insoluble fission products. In the degradation process, enlargement of the leakage path and exposure of fuel pellets to flowing coolant leads to oxidation and mass transfer (washout) of fuel particles from the damaged rod to the primary coolant system. These dispersed fuel particles, generally called “tramp uranium”, can stick to the surfaces of fuel rods and other primary system components. The particles that deposit in the core continue to fission and release radionuclides directly to the coolant. Depending on the extent of degradation and the amount of fuel washout, long-term activity increases due to tramp uranium can be significantly larger than the steady-state increase from a leaking rod prior to degradation. The increase due to washout continues after the degraded rod has been removed from the core. Activity due to tramp uranium decreases in rough proportion with the fraction of the affected fuel assemblies that are discharged each reactor cycle; e.g., 6 – 10 years to return to pre-degradation activity levels. So, another significant component of the failure cost arises from the long term increase in exposure levels and action necessary to mitigate their effects.

The Executive Board of the Institute of Nuclear Power Operations (*INPO*) set the goal of eliminating fuel failures in all U.S. plants by 2010, *INPO*, 2007. The Chief Nuclear Officers of U.S. utilities have since pledged their support. While the feasibility of "zero leakers" as opposed to "as low as reasonably achievable" remains to be established, an integrated approach by suppliers, operators and regulators to achieving ultra-high reliability fuel is expected to benefit operational, cost and exposure issues. A key factor in such an approach is the examination and analysis of irradiated fuel at reactor sites, in hot cells and in related laboratories. Thus, to make progress toward ultra-high reliability fuel and to reduce the potential for post-failure degradation, it is imperative to examine failed and non-failed fuel. The most cost efficient way to carry out these examinations is to begin with a good understanding of the known mechanisms of failure and degradation and of the principal methods for examining irradiated fuel. With such an understanding, fuel investigation and development programs can be focused on the likely causes of failure or degradation, while unnecessary costly and time consuming work can be minimized. One of the objectives of this Handbook is to provide such an understanding.

For reference, a brief summary of fuel failures mechanisms is given in Table 5-1. Failures due to the first two causes, manufacturing defects and cladding collapse, are relatively infrequent. The exception is pellets with chips or missing pellet surface. Such pellets have been involved in recent *PCI* failures and are the object of ongoing manufacturing development. Another potential exception is primary hydriding. Failures due to primary hydriding were effectively eliminated by the introduction of fuel pellets with little or no open porosity and by the exclusion of moisture and other hydrogen-bearing material from the inside of fuel rods during the final assembly process. However, the underlying risk still exists and could lead to fuel failures in the event of an undetected excursion in moisture contamination. Fuel failures due to excessive cladding corrosion are also relatively infrequent. Corrosion failures typically result from a common cause or a set of causal factors and can affect a large number of rods in a given reload or core. The rate of *PCI* failures was greatly reduced by the use of zirconium liners, but appears to be increasing with more demanding core loadings and operating cycles; i.e., longer cycles, more rods at the upper end of the design range, larger power ramps to high powers after longer times at low power. As noted in Table 5-1, some of the recent duty-related failures have also involved pellets with missing cylindrical surface. Cladding perforation due to fretting remains as the leading recurrent failure mechanism. Fretting due to the trapping of foreign material next to fuel rods is a source of failures in both *BWR*s and *PWR*s. The frequency of failures due to debris fretting varies among reactors, ranging from none in some plants to multiple rods in multiple cycles in other plants. The frequency of such failures is decreasing, however, due to debris filters in fuel bundles, strainers in feedwater lines and debris exclusion practices by the fuel suppliers and reactor operators. Fretting due to fuel rod vibration relative to spacer grids is a problem unique to some *PWR* fuel designs and plants.

Table 5-1: Summary of *LWR* failure mechanisms.

Primary Failure Cause	Short Description
Manufacturing defects	Non-through-wall cracks in the fuel cladding developed during the cladding manufacturing process. Moisture in fuel pellets and/or contamination of clad inner surface by moister or organics that leads to primary hydriding. Too large gap between the fuel rod and the spacer grid supports (poor spacer grid manufacturing process) leading to excessive vibrations in the *PWR* fuel leading to fretting failures. Chipped pellets and pellets with "missing surfaces" may result in *PCI* failures both in *BWR* liner and non-liner fuel as well as *PWR* fuel.
Cladding collapse	This failure mechanism occurred due to pellet densification. This failure mode has today been eliminated by fuel design changes and improved manufacturing control.
Excessive corrosion	An accelerated corrosion process that results in cladding perforation. Accelerated corrosion can result from a number of factors; e.g., *CRUD* deposition (CILC or thermal blanketing), *ESSC*, (in *BWR*s), dry-out due to excessive *FA* bowing, abnormal cladding chemistry or microstructure, coolant chemistry upsets. Failures due to excessive corrosion are now infrequent, but can involve a large number of rods when such an event occurs.
PCI	*PCI*-an iodine assisted stress corrosion cracking or liquid metal embrittlement phenomenon that may result in fuel failures during rapid power increases in a fuel rod. There are three components that must occur simultaneously to induce *PCI*; viz., 1) tensile stresses- induced by the power ramp, 2) access to freshly released iodine-occurs during the power ramp, provided that the fuel pellet temperature becomes large enough and 3) a sensitised material – Zircaloy is normally sensitive enough for iodine *SCC* in unirradiated state (susceptibility greatest in cold worked material) or after irradiation hardening. The *PCI* failure mechanism occurred primarily in *BWR*s, but was essentially eliminated by the introduction of zirconium barriers. The incidence of *PCI* failures has increased in the past few years with longer operating cycles, an increased fraction of the fuel rods in a core operating at high power and larger power increases after longer intervals at low power. Missing pellet surface has also been a factor in some of the recent duty-related failures.
Fretting	This failure mode has occurred due to: • Debris fretting in *BWR* and *PWR* • Grid-rod fretting - Excessive vibrations in the *PWR* fuel rod causing fuel failures. This situation may e.g. occur due to different pressure drops in adjacent fuel assemblies causing cross-flow. • Baffle jetting failures - Related to high coolant cross-flows close to baffle joints in some *PWR*s. Fretting is now the leading recurrent cause of fuel failures in both *BWR*s and *PWR*s

6 Maintaining good fuel reliability, *HFE*

As mentioned earlier, another reason for poolside examinations of non-defected fuel is to maintain good fuel reliability, i.e., make sure that no fuel related issues occur.

In most cases there are two types of poolside examinations to meet this objective, namely:

1) Visual examinations and
2) measurements of:
   a) the dimensions of the *FA* and its components (this may of course also be assessed by visual examinations,
   b) oxide thickness of Zr alloys components (fuel rods, guide tubes, spacers, fuel outer channels, etc.),
   c) *CRUD* thickness and composition.

The mechanisms of dimensional changes of *FA* components, including the parameters impacting the dimensional changes, are rather well known and are discussed in Section 3.3.5. For this reason, information on *HFE*s, related to dimensional changes is not repeated in this Section Instead this section focuses on the corrosion issue, the reasons being:

- Knowledge about the reasons for corrosion failures is still lacking[27].
- When corrosion failures occur they tend to do so in large numbers if water chemistry/*CRUD* is involved.
- Corrosion failures results in large activity release and can lead to significant fuel washout.

One of the primary reasons for a utility to carry out *HFE*s is to track the effectiveness of water chemistry management practices, particularly when changes in water chemistry strategy are being considered; e.g. implementing or changing the rate of Zn-injection. The practice of conducting well structured *HFE*s on a regular basis provides a baseline for the corrosion performance of fuel assemblies in a given reactor and operating environment. It also provides a means for assessing the effects of water chemistry or fuel material changes on corrosion performance and for detecting potentially deleterious effects before they become reliability issues. To establish the baseline data it is important to examine fuel that has been exposed to the "old water chemistry" for various burnups. Figure 6-1 gives an example where fuel irradiated

- 1 cycle with "old chemistry"
- 2 cycles with "old chemistry"
- 3 cycles with "old chemistry"
- 4 cycles with "old chemistry"
- 5 cycles with "old chemistry"

forms the baseline data while the same fuel rods are measured again after the water chemistry change was implemented. The figure shows that in this case the change in water chemistry resulted in a small increase in corrosion rate that increased with burnup. Such information will help the utility to get an early warning of a potential reliability issue.

[27] To clarify this statement, a large body of knowledge exists regarding water chemistry, material science and corrosion. Experts in these areas have established guidelines and are usually able to reach a consensus regarding the reason for corrosion failures after the fact. They have, however, been unable to identify conditions that led to corrosion failures before the fact in a number of significant events.

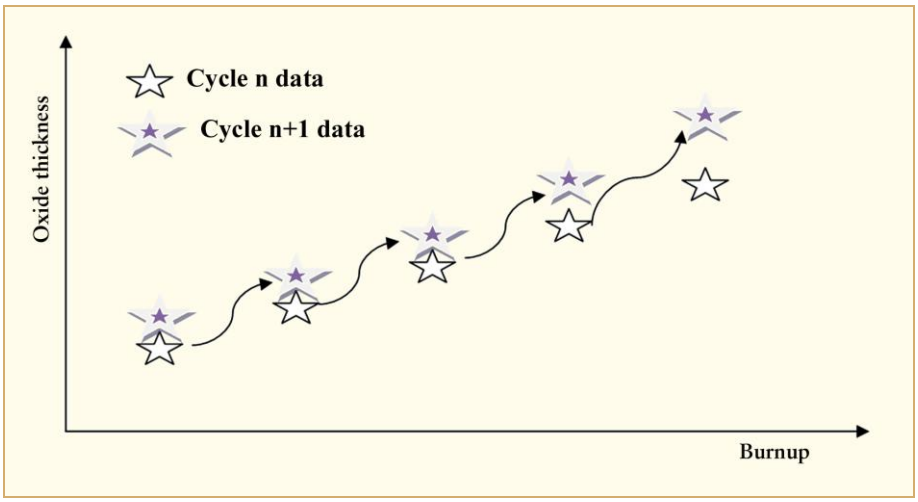

Figure 6-1: Figure showing schematically the data before and after a change has been introduced; e.g., in water chemistry. The arrows indicate that the representative samples from each reload batch are measured before and after the change in water chemistry. In this case, a small increase in corrosion rate can be seen after the change.

When *HFE*s are performed, it is recommended that all important parameters having an impact on corrosion performance be characterised and that all of this information go into the Fuel Examination Report; i.e., the report that documents the results of the fuel poolside examination[28]. The advantage of such a Report is that it will hopefully contain sufficient information to explain the reasons for a potential increase in corrosion rate later on. It is also much easier to put together the relevant characterisation data at the time of the Poolside Examinations instead of doing this several years afterwards if it turns out that the corrosion performance is not as expected. Below is a list of recommended information to be included in the Poolside Examination Report:

- Initial fuel rod and material characteristics from drawings and vendor specifications or certifications applicable to the respective fuel assemblies. Note, however, that the actual characteristics of the rods being examined will be somewhat different from the nominal values in the drawings and specifications so that a large sample size and statistical methods are generally needed to improve resolution of the *HFE*s. The initial characteristics of interest include:
  - Chemistry of the fuel cladding (in case of liner/barrier – also chemistry of the liner/barrier, specifically the Fe content is important for fuel degradation purposes) – in most cases only the ingot chemistry is available which may differ significantly from that in the actual fuel rod.
    - Corrosion performance depends on the material microstructure, which is a function of chemistry and manufacturing process.
  - General information on manufacturing process being used. Most fuel vendors have categorised their manufacturing process that have been used over time a number or other alphanumeric designation; e.g., Process 7 (*GNF*) or *LK*3 (Toshiba-Westinghouse).
    - See bullet above.

[28] Measurements related to poolside examinations are frequently performed at an off-site laboratory and documented in a separate report; e.g., *CRUD* composition. It is important to document the details of such samples and measurements so that the poolside inspection and subsequent laboratory reports can be confidently linked to specific measurement campaigns, fuel assemblies, rods, axial locations and water chemistry conditions.

  - Length and diameter of fuel rod cladding,
    - An excessive increase in fuel rod length is often related to large hydrogen pickup during the corrosion process.
    - Changes in cladding diameter and liftoff due to *CRUD* and oxide are direct indications of the effects of water chemistry on corrosion. Although the plenum regions are frequently used as reference points for such changes, specific data are available from the *QA* systems of some fuel suppliers and should be included in the examination report when possible.

- Reactor operation information for the whole lifetime of the fuel rod(-s) that comprise the *HFE*s; i.e.
  - Core position of the examined *FA*(-ies) and information about its neighbouring assemblies – specifically important in *PWR*s.
    - In *PWR*s where the Zr alloy corrosion rate is very much dependent on the material temperature, the power of the rods in adjacent fuel assemblies my impact the temperature (and degree of boiling) in the periphery row of fuel rods in the *FA* being examined.
  - Power history - The detailed rod power history is not an essential part of a poolside inspection report, but should be somehow captured and recorded when the needed data are still available in the process computers. As a minimum, the examination report should include the assembly average exposures and cycle exposure increments or information to readily calculate such data; e.g., the ratio of the *FA* average burnup increase /core average *FA* burnup.
    - In *PWR*s, the power history resulting in the largest oxide thickness at discharge involves continuously increasing rod power with burnup.
    - In *BWR*s, it is not clear which power history gives the largest oxide thicknesses at discharge. There is, however, an impact of power history and in some cases a "high-low-high" power history may give the largest oxide thicknesses.
    - It is recommended that fuel rods with similar burnups but 2-4 different power histories are investigated.
  - Cycle length and burnup increase per cycle.
  - Coolant inlet temperature (*PWR*s/*VVER*s).
    - Increasing inlet temperature will increase fuel rod temperature with all other conditions held constant.
  - Water chemistry strategy being applied.
    - This could be information such as *HWC*, noble metal chemistry (NMC), Fe and/or Zn injection in *BWR*s.
    - Or, this could be information such as maximum LiOH/pH, maximum boron concentration, Zn injection in *PWR*s.
  - Bulk coolant chemistry measured by grab and integrated sampling.
  - Duty Index or similar information for *PWR*s/*VVER*s to indicate if and, if so, how much boiling occurs at the water/fuel cladding tube interface.
    - More subcooled boiling results in larger enrichments of soluble species in the remaining coolant after the steam bubbles have left. The enrichment factor also increases with the thickness of the *CRUD* and oxide layer if subcooled boiling occurs.

7 *FA* characterisation techniques

The performance of the different *FA* components may be characterised by examinations performed in the pool or in a hot cell facility[29], Figure 7-1. The examinations in pool are usually non-destructive, but can also involve destructive operations such as breaking a flow tab off of a spacer or cutting coupons from a channel for measurement of hydrogen concentration. As discussed in the section on fuel rods, hot cell examinations normally start with non-destructive followed by destructive examinations. The costs for hot cell examinations are much more expensive than those carried out in pool. However, certain material characteristics can only be assessed in a hot cell. In the following subsections examples of different examination techniques and results obtained are discussed.

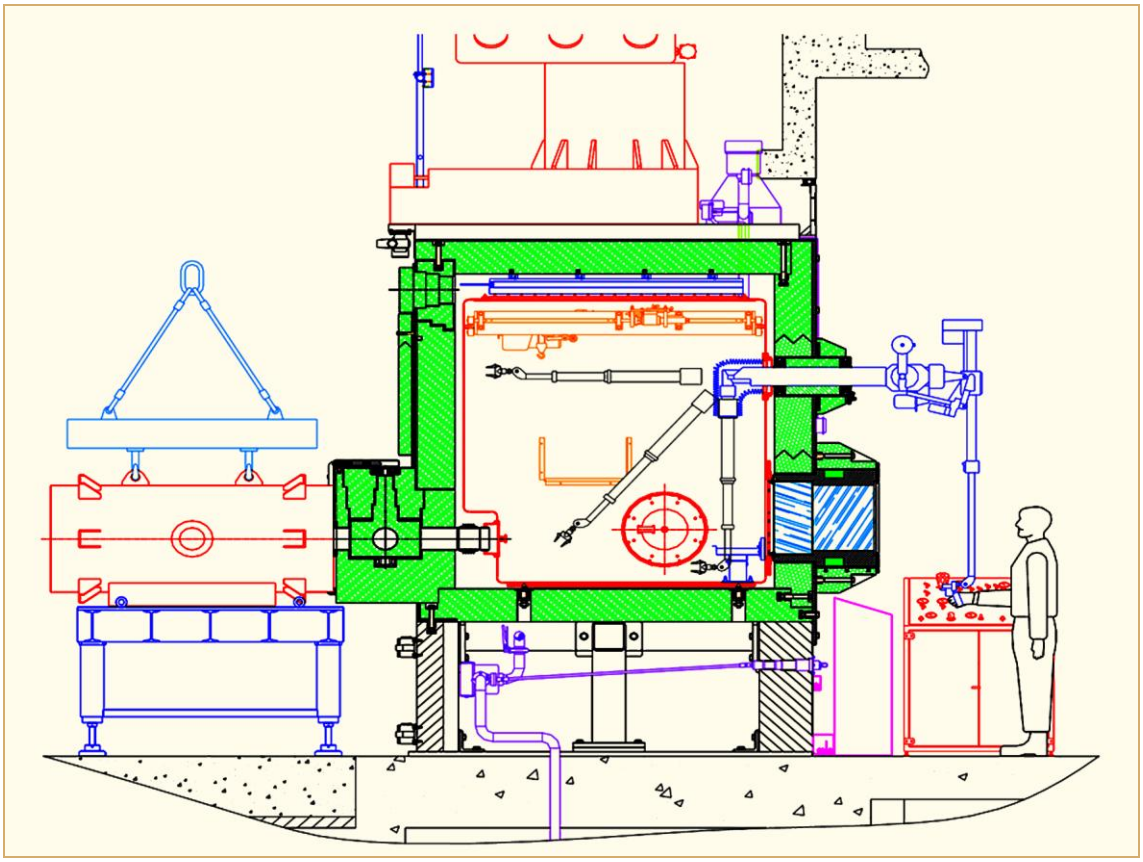

Figure 7-1: Schematic showing a Hot Cell, Yvon, 2006.

[29] Shielded containments are commonly referred to as Hot Cells. The word "hot" being used as a synonym for radioactive. Hot cells are used in both the Nuclear and the Nuclear Medicines Industry. They are required to protect individuals from radioactive isotopes by providing a safe containment box in which they can control and manipulate the equipment required. Hot cells are used to inspect spent nuclear fuel rods and to work with other items, which are high-energy gamma ray emitters.

7.1 *FA* outer flow channel (*BWR*)

Various poolside equipment can be used to determine the dimensions of the outer flow channel of *BWR* fuel assemblies. Figure 7-2 shows a schematic of a system, which utilizes *LVDT*s, to measure the position of a channel relative to a reference surface. In this case, each of the four sides is measured by three transducers and consequently 12 axial traces are obtained simultaneously over the circumference of the channel. From these measurements, the bulge, bow, and twist may be calculated over the total length of the channel.

The dimensions of the outer flow channels are of interest in the performance of individual *BWR* fuel assemblies and in the interaction of the bundles comprising a control cell with each other and with their control blade. Bulge is a measurement of the out-of-plane deformation of the channel faces. Bulging results from the difference in pressure between the inside and the outside of the flow channel and from the effects of fast neutrons on channel creep. Bulging can also result from the force of mechanical seals that are used in some designs to reduce the bypass leakage between the channel and lower support plate. The pressure differential and seal force is greatest at the bottom of the flow channel and vanishes at the top of a *FA*. The fast neutron flux varies with operating conditions, but is relatively small at the bottom of a *FA*, increases with elevation and void fraction and then decreases due to flux leakage near the upper end of an assembly. The net result is an outward deformation that is greatest at the transverse centre of each face near the lower end of a fuel channel and varies with axial position along the length of a channel. Such outward deformation of a channel is of interest because of its potential effects on the leakage of coolant into the bypass region outside of the channel and on the interference with the movement of adjacent control blades.

As shown in Figure 7-2, channel bow is a lateral deformation relative to an idealized centreline of the *FA*. Twist is an angular deformation over the length of an assembly. A *BWR FA* without internal flow channels is sufficiently flexible that it follows the bow and twist of its outer channel. Part of both types of deformation typically results from the effects of temperature and fast neutrons on stress relaxation and irradiation growth. Residual stress from manufacturing operations can cause a channel to deform due to thermal and fluence induced relaxation. The texture and residual, as-built microstructure of zirconium-based alloys can contribute to significant amounts of lateral deformation due to the effects of fast neutron fluence and fluence gradients on the differential irradiation growth among channel faces. Another part of channel bow results from shadow corrosion that has been observed to lead to differences in the pickup of hydrogen and differential growth among channel faces. For both irradiation and corrosion induced bow, a channel bows outward away from its centreline on the face with the largest growth. Lateral growth is of interest due to its potential effects on the motion of adjacent control rods, on local increases in thermal neutrons and, in extreme cases, on the width of flow passages between the channel and fuel rods.

The length of the fuel channel is also of interest and can be measured with systems similar to that shown in Figure 7-2 when equipped with the appropriate sensors. Length can also be determined by means of in-pool devices that range from tape measures to calliper-like gages equipped with *LVDT*s or similar sensors. Length data are used to assess the effects of differential growth in the axial direction on the fit and remaining growth margin of the channel relative to its fuel bundle. Length data can also be used to estimate lateral bow in cases where time or equipment availability prevents more accurate, explicit measurements.

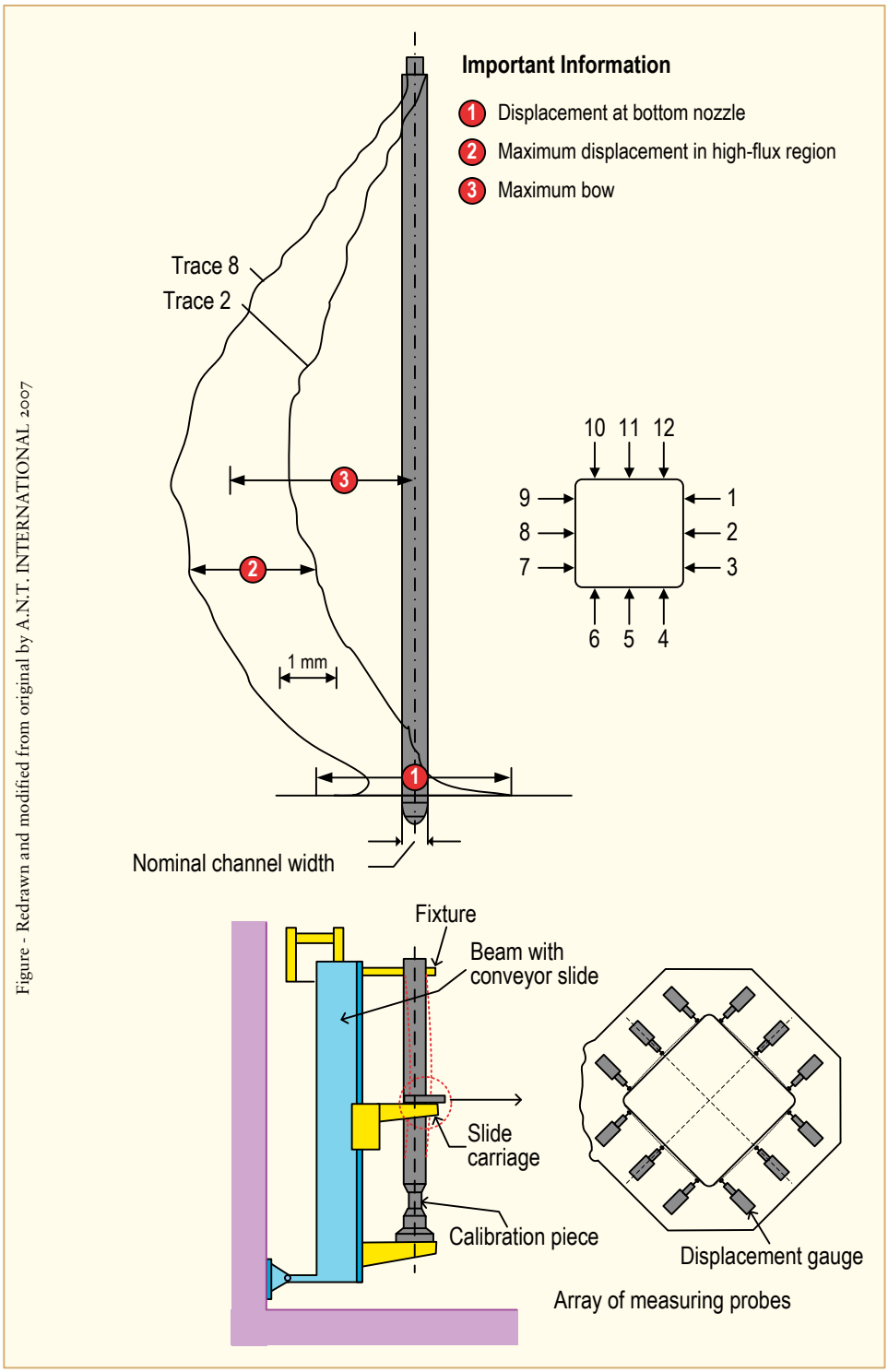

Figure 7-2: Schematic view of the channel measurement device and typical measurement results, Knaab & Knecht, 1978.

8 References

Adamson R., Cox B., Rudling P., Strasser A. and Wikmark, "*The Annual Review of Zirconium Alloy Technology for 2000*" *ZIRAT5/IZNA1* Annual Report, Advanced Nuclear Technology, 2000.

Adamson R. B. and Rudling P., "*Mechanical Properties of Zirconium Alloys*", *ZIRAT6/IZNA1* Special Topical Report, *ANT* International, November, 2001/2002.

Adamson R. B. and Rudling P., "*Dimension Stability of Zirconium Alloys*", *ZIRAT7/IZNA2* Special Topical Report, *ANT* International, 2002/2003.

Adamson R. B., Cox B., Garzarolli F., Strasser A., Rudling P. and Wikmark G., "*Corrosion of Zirconium Alloys*", *ZIRAT7/IZNA2* Special Topical Report, *ANT* International, 2002/2003.

Adamson R. B., Cox B., Garzarolli F., Strasser A., Rudling P. and Wikmark G., "*High Burnup Fuel Issues*", *ZIRAT8/IZNA3* Special Topics Report, *ANT* International, 2003/2004.

Adamson and Cox, "*Impact of Irradiation on Material Performance*", *ZIRAT10/IZNA5* Special Topics Report, *ANT* International, Skultuna, Sweden, 2005/2006.

Adamson R., Cox B., Davies J., Garzarolli F., Rudling P. and Vaidyanathan S., "*Pellet-Cladding Interaction (PCI and PCMI)*", *ZIRAT11/IZNA6*, Special Topical Report, *ANT* International, 2006/2007.

Adamson R., Garzarolli F., Cox B., Strasser A. and Rudling P., "*Corrosion Mechanisms in Zirconium Alloys*", *ZIRAT12/IZNA7* Special Topic Report, *ANT* International, 2007/2008.

Anderson T., Almberger J and Björnkvist L., "*A Decade of Assembly Bow Management at Ringhals*", ANS Topical Meeting on Light Water Reactor Fuel Performance, Orlando, Fl., 2004.

Baily W. E., et al., Proc. ANS Top. Meeting LWR Fuel Performance, Avignon, France, p. 26-35, Apr. 21-24, 1991.

Barberis P., Rebeyrolle V., Vermoyal J.J., Chabretou V. and Vassault, J.P., "*CASTA DIVTM: experiments and modeling of oxide induced deformation in nuclear components*", 15th ASTM International Symposium: Zirconium in the Nuclear Industry, Sun River, OR, June 2007.

Beier P. Dewes P. and Hoffmann, "*Methods for examination of BWR fuel assembly structure exemplified by the implementation of Zry-2 PGP+ as material for structural components*", Fachtagung der KTG-Fachgruppe, Brennelemente und Kernbauteile, 2008.

Beuneche D., Bordly M., Bournay P., Pelletier J., Pattat D. and Warlop R., "*Overview of Fuel Sipping in French Power Plants*", ANS International Technical Meeting on LWR Fuel Performance, Virginia, USA, 1988.

Cheng Bo, Smith David, Armstrong Ed, Turnage Ken and Bond Gordon "*Water chemistry and Fuel performance in LWRs*", Proc. Int'l Topical Meeting *LWR* Fuel Performance, Park City, UT, April 10-13, 2000, Vol. 1, 355-371, 2000.

Cox B., "*Pellet-Clad Interaction (PCI) failures of Zirconium alloy fuel cladding – a review*", Journal of Nuclear Materials 172, pp. 249-292, 1990.

Cox B. and Rudling P., "*Hydriding Mechanisms and Impact on Fuel Performance*", *ZIRAT5*, Special Topic Report, Advanced Nuclear Technology, 2000.

Cox B., Garzarolli F., Strasser A. and Rudling, P., "*The Effects of Zn Injection (PWRs and BWRs) and NobleMetal Chemistry (BWRs) on Fuel Performance - an Update*", *ZIRAT8/IZNA3* Special Topical Report, *ANT* International, 2003/2004.

Cox B., Garzarolli F., and, Rudling R., "*Corrosion of Zr-Nb Alloys*", *ZIRAT9/IZNA4* Special Topics Report, *ANT* International, 2004/2005.

Cox B., Garzarolli F., Strasser A. and Rudling P., "*Structural Behaviour of Fuel and Fuel Channel Components*", *ZIRAT10/IZNA5* Special Topical Report, *ANT* International, 2005/2006.

Cox B., Garzarolli F., Adamson R., Rudling P. and Strasser A., "*Fuel Material Technology Report, Vol. 1*", *ANT* International, 2006.

Dust M., Langenberger J., Habeck K., Stark R., Beier M., "*Detecting Small Flaws in Fuel Rods with Sophisticated Eddy Current Testing and Single Rod Sipping*", Fachtagung der KTG-Fachgruppe, Brennelemente und Kernbauteile, 28 – 29 October 2008, papers 2a and 2b, 2008.

EPRI Guidelines: Fuel Surveillance and Inspection, Product 1015032, 2008.

Ferguson Scott D., Davis Dennis D., Correal-Pulver Olga, Seel David, "*Post Irradiation Examination of the Lead Westinghouse Robust Fuel Assemblies after Three Cycles of Operation in the Wolf Creek Generating*", Proc: ENS TopFuel 2003, Würzburg, Germany, 2003.

Franklin D. G. and Adamson R. B., "*Implications of Zircaloy creep and growth to light water reactor performance*", J. Nucl. Materials 159, pp. 12-21, 1988.

Fukuya et al., "*BWR Fuel Channel Performance and Localized Corrosion at High Burnups*", Proc. ANS *LWR* Fuel Performance Conference, Palm Beach, pp. 580-586, 1994.

Garlick A., "*Stress Corrosion Cracking of Zircaloy in Iodine Vapour*", UK Report, TRG Memo 4336(W), 1968.

Garlick A. "*A critical review of available information on fuel failures in Douglas Point and some AECL loop experiments*", UK Report, TRG Memo 5002(W), 1969.

Garzarolli F., Manzel R., Peehs M and Stehle H., "*Observations and hypothesis on pellet-clad interaction failures*", Kerntechnik 20 Jahrestagung, No. 1, pp. 27-31, 1978.

Garzarolli F., Von Jan R. and, Stehle H., "*The main causes of fuel element failure in water cooled power reactors*", Atomic Energy Review, Vol. 17, pp. 31-128, 1979.

Garzarolli F., Stehle H., Steinberg, E., "*Behavior and Properties of Zircaloys in Power Reactors: A Short Review of Pertinent Aspects in LWR Fuel*", Zirconium in the Nuclear Industry: 11th Int'l Symposium, ASTM STP 1295, Bradley E. R. and Sabol G. P., Eds., American Society for Testing and Materials, 12-32, 1996.

Garzarolli F., "*Development of cladding materials for BWR and PWR fuel*", 10th Int. Conf, Environmental Degradation of Materials in Nuclear Power Systems-Water Reactors, Lake Tahoe Nevada., August 5-9, 2001.

Garzarolli F., et al., "*Corrosion Phenomena in Zr Alloy Fuel Claddings at High Burnups*", 10th Int. Conf, Environmental Degradation of Materials in Nuclear Power Systems-Water Reactors, Lake Tahoe Nevada., August 5-9, 2001.

Gorman J. A. and Lipsey G. W., "*An Assessment of BWR Fuel Channel Lifetimes*", EPRI-Report NP-2483, 1982.

Groeschel F. (PSI), Yagnik S. (EPRI), "*Primary Failure Features in Zr-lined BWR Fuel*", 31st International Utility Fuel Performance Meeting, New Orleans, LA, August 13-15, 2001.

Groeschel F., Bart G., Montgomery R., Suresh K. Yagnik, "*Failure Root Cause of a PCI Suspect Liner Fuel Rod*", *IAEA* Technical Meeting on Fuel Failure in Water Reactors: Causes and Mitigation, Bratislava, Slovakia, 17-21 June 2002.

Hayashi H., Shimada S. and Sakurai H., "*Outside-in Failure of High Burnup BWR Segment Rods Caused by Power Ramp Test*", Proc. ENS Top Fuel, Würzburg, Germany, 2003.

Hayashi H., Ogata K. and Kamimura K., "*Outside-in Failure of High Burnup Fuel Cladding and Evaluation Tests of the Mechanism*", Water Reactor Fuel Performance Meeting, paper 1080, Kyoto, Japan, 2 – 6 October, 2005.

Hessler O., "*Ultrasonic Testing and Moulding Technique for Fuel Element Inspection*", KTG Fachtagung, Brennelemente und Kernbauteile, 28-29 October,, paper 3, 2008.

IAEA, *Review of Fuel Failures in Water Cooled Reactors*, Technical report series no. 388, *IAEA*, Vienna, 1998.

INPO, "Guidelines for Achieving Excellence in Nuclear Fuel Performance", INPO 07-004, June 2007.

Jang Young Ki, Kim Jae Ik, Kim Kyu Tae, Lee Chong Chul and Park Chan Oh, "*In-Reactor Verification Of Advanced Nuclear Fuel, PLUS7TM, for KSNPS*", Proceedings of the 2007 International *LWR* Fuel Performance Meeting San Francisco, California, September 30 – October 3, 2007.

Jenssen H.K. and Oberländer B.C., "*Neutron radiography, three dimensional profilometry and image compilation of PIE data for visualization in an image based user-interface*", *IAEA*-TECDOC-1277, Advanced post-irradiation examination techniques for water reactor fuel Proceedings of a Technical Committee meeting held in Dimitrovgrad, Russian Federation, 14-18 May 2001.

Kim Yong-Soo, Lee Myung-Chan, Kim Kyoung-Doek, Myung-Jae Song Yong-Bum Chun, You Gil-Sung, Min Duck-Kee, Eun-Ka Kim Hwee-Soo Jun, Suh Doo-Suhk, Park Hyun-Taek, Jang-Hee Hong, "*Hydriding Failure Analysis Based on Pie Data*", Proc: ANS-2000, Park City, Utah, USA, 2000.

King S., Kesterson R., Yueh K., Comstock R., Herwig W.and Ferguson S., "*Impact of Hydrogen on the Dimensional Stability of ZIRLO Fuel Assemblies",* ASTM STP 1423, 2002.
Kitano Koji, Losin Carolina, Arborelius Jakob and Limbäck Magnus, "*Study on incipient cracks at inner surface of cladding liner after high power irradiation test*", Proc. Water Reactor Fuel Performance Meeting, pp. 268-275, Kyoto, Japan, October 2-6, 2005.
Knaab H and Knecht K., "*Pool Site Fuel Inspection and Examination Techniques Applied by the KWU Fuel Service*", Proc. 26th Conference on Remote System Technology, 1978.
Knecht K., Stark R. and Habeck K., "*In-Core Sipping at BWR Plants in Only 16 Hours*", Top Fuel 2001, paper 2-24, 2001.
Kratzer A., et al., "*Experience and Development Trends of BWR Fuel Channels*", Jahrestagung Kerntechnik, Köln, 1993.
Ledergerber Guido., Abolhssan Sousan, Limbäck Magnus, Lundmark Roger J. and Magnusson Kurt-Åke, "*Characterization of High Burnup Fuel for Safety Related Fuel Testing*", Journal of Nuclear Science and Technology, Vol. 43, No. 9, p. 1006–1014, 2006.
Ledergerber G., Kaufmann W., Ritter A., Greiner D., Parmar Y., Jacot-Guillarmot R. and Krouthén J., "*Burnup Increase and Power Uprate – Operation History of KKL"*, Int. *LWR* Fuel Performance Meeting, San Francisco, California, September, 2007.
Lemons J., "*Fuel Assembly Inspection Program*", Nuclear Plant Journal, January-February 2008.
Limbäck M., Dahlbäck M., Tägtström P, Jourdain P, Massih A., Sihver L, Andersson T and Witt P., "*Westinghouse Optimised BWR Cladding and Channel Materials*", Proc: ENS, Top Fuel, Stockholm, Sweden, May, 2001.
Lin C.C., Radiochemistry in Nuclear Power Reactors, National Research Council, Nuclear Science Series, NAS-NS-3119, National Academy Press, Washington, D.C., 1996.
Lysell G., Blomberg B., Calesson L.P., Brandes and Skusa J., "*Failure Root Cause Identification at Studsvik*", Fachtagung der KTG-Fachgruppe, Brennelemente und Kernbauteile, 28/29 October 2008.
Meek M.E. and Rider B.F., "*Compilation of Fission Product Yields, Vallecitos Nuclear Center, 1974*", GE Report NEDO-12154-1, January 26, 1974.
Mahmood S.T., Lin Y-P, Dubecky M.A., Edsinger K. and Mader E.V., "*Channel Bow in BWRs-Hot Cell Examination Results and Correlation to measured Bow*", Proceedings of the 2007 International *LWR* Fuel Performance Meeting, San Francisco, CA, paper 1061, 2007.
Mardon J. P. and Leger A. C., "*Performance of M5 Alloy as Cladding Tube and Structural Component Material*", 18th KAIF/KNS Annual Conference, April 9-11, 2003.
Mardon J.P., Hoffmann P.B., Garner G.L., "*High Burnup Behavior and Licensing of Alloy M5*", Proceedings of the 2005 International Meeting on *LWR* Fuel Performance Kyoto, Japan, October 2-6, 2005.
NEA/CSNI, "*Fuel Safety Criteria In NEA Member Countries, March 2003*", Nuclear Energy Agency, Committee On The Safety of Nuclear Installations, *NEA*/CSNI/R(2003)10, 17 July 2003.
Nikulina A., Shishov S., Cox B., Garzarolli F. and Rudling P., "*Manufacturing of Zr-Nb Alloys*", *ZIRAT11/IZNA6* Special Topic Report, *ANT* International, 2006/2007.
Ozer O., EPRI's Failed-Fuel Degradation Program, Proc. Failed Fuel Degradation Workshop, Palo Alto, 1995.
Piascik T. and Kasik P., "*Fuel Channel Oxide Thickness Measurement at Oyster Creek Nuclear Generating Station*", *IAEA* Techn. Committee Meeting on Fundamental Aspects of Zirconium-Base Alloys in Water Reactor Environments, Portland, 1989.
Potts G. A. and Proebstle R. A., "*Recent GE BWR fuel experience*", Light Water Reactor Fuel Performance (Proc. Int. Top. Mtg. West Palm Beach, FL, 1994), American Nuclear Society, LaGrange Park, IL, 87, 1994.
Poussard C., Averty X., Duguay O., Rabouille O., Le Saux M., Pizzanelli J., Dumas C., Genisson M., Le Breton M., Sainte Catherine C. and Yvon P., Technical Seminar on Effects of Irradiation in Materials, Saclay, France, 09/2006.
Powers Chris, Dewes Peter, Billaux Michel, Perkins Richard, Ruzauskas Ed, Armstrong Ed, Ralph Richard, Blomberg Göran, Lysell Gunnar and Cheng Bo, "*Hot Cell Examination Results of Non-Classical PCI Failures at La Salle*", Proc. Water Reactor Fuel Performance Meeting, Kyoto, Japan, October 2-6, 2005.
Riess R and Lundgren K., "*CRUD in PWR/VVER and BWR Primary Circuits*", *LCC2* Special Topic Report, *ANT* International, Skultuna, Sweden, 2006.